NAVAL POSTGRADUATE SCHOOL

MONTEREY, CALIFORNIA

THESIS

NEW PULSE SHAPES FOR ENHANCED SPECTRAL EFFICIENCY IN DIGITAL RADIO COMMUNICATIONS

by

Nga Chee Wei

September 2007

Thesis Advisor:	Frank Kragh
Second Reader:	Roberto Cristi

Approved for public release; distribution is unlimited

THIS PAGE INTENTIONALLY LEFT BLANK

REPORT DOCUMENTATION PAGE			Form Approved OMB No. 0704-0188
Public reporting burden for this collection of information is estimated to average 1 hour per response, including the time for reviewing instruction, searching existing data sources, gathering and maintaining the data needed, and completing and reviewing the collection of information. Send comments regarding this burden estimate or any other aspect of this collection of information, including suggestions for reducing this burden, to Washington headquarters Services, Directorate for Information Operations and Reports, 1215 Jefferson Davis Highway, Suite 1204, Arlington, VA 22202-4302, and to the Office of Management and Budget, Paperwork Reduction Project (0704-0188) Washington DC 20503.			
1. AGENCY USE ONLY *(Leave blank)*	**2. REPORT DATE** September 2007	**3. REPORT TYPE AND DATES COVERED** Master's Thesis	
4. TITLE AND SUBTITLE New Pulse Shapes for Enhanced Spectral Efficiency in Digital Radio Communications		**5. FUNDING NUMBERS**	
6. AUTHOR(S) Nga Chee Wei			
7. PERFORMING ORGANIZATION NAME(S) AND ADDRESS(ES) Naval Postgraduate School Monterey, CA 93943-5000		**8. PERFORMING ORGANIZATION REPORT NUMBER**	
9. SPONSORING /MONITORING AGENCY NAME(S) AND ADDRESS(ES) N/A		**10. SPONSORING/MONITORING AGENCY REPORT NUMBER**	
11. SUPPLEMENTARY NOTES The views expressed in this thesis are those of the author and do not reflect the official policy or position of the Department of Defense or the U.S. Government.			
12a. DISTRIBUTION / AVAILABILITY STATEMENT Approved for public release; distribution is unlimited		**12b. DISTRIBUTION CODE**	

13. ABSTRACT (maximum 200 words)

Linear modulation schemes such as phase shift keying (PSK) and quadrature amplitude modulation (QAM) are inherently spectrally efficient. This research seeks enhanced spectral efficiency by designing new spectrally efficient pulse shapes for such digital modulations. The pulses designed are of finite duration and exhibit zero intersymbol interference when received through an additive white Gaussian noise (AWGN) channel. It is shown that the resulting communications signals have optimal spectral roll-off while maintaining optimum bit error ratio performance when received via an AWGN channel. The bandwidths and power spectral densities of communications signals using these pulses are compared with traditional spectrally efficient communications signals.

14. SUBJECT TERMS Nyquist Pulse, Spectral Efficiency, Intersymbol Interference, Additive White Gaussian Noise (AWGN).			**15. NUMBER OF PAGES** 87
			16. PRICE CODE
17. SECURITY CLASSIFICATION OF REPORT Unclassified	**18. SECURITY CLASSIFICATION OF THIS PAGE** Unclassified	**19. SECURITY CLASSIFICATION OF ABSTRACT** Unclassified	**20. LIMITATION OF ABSTRACT** UU

NSN 7540-01-280-5500 Standard Form 298 (Rev. 2-89)
Prescribed by ANSI Std. 239-18

THIS PAGE INTENTIONALLY LEFT BLANK

Approved for public release; distribution is unlimited

NEW PULSE SHAPES FOR ENHANCED SPECTRAL EFFICIENCY IN DIGITAL RADIO COMMUNICATIONS

Chee Wei Nga
Project Manager, Defence Science and Technology Agency
B. Eng, Nanyang Technological University of Singapore, 1998
M. Sci, National University of Singapore, 2002

Submitted in partial fulfillment of the
requirements for the degree of

MASTER OF SCIENCE IN ELECTRICAL ENGINEERING

from the

NAVAL POSTGRADUATE SCHOOL
September 2007

Author: Chee Wei Nga

Approved by: Assistant Professor Frank Kragh
Thesis Advisor

Professor Roberto Cristi
Second Reader

Professor Jeffery B. Knorr
Chairman, Electrical and Computer Engineering Department

THIS PAGE INTENTIONALLY LEFT BLANK

ABSTRACT

Linear modulation schemes such as phase shift keying (PSK) and quadrature amplitude modulation (QAM) are inherently spectrally efficient. This research seeks enhanced spectral efficiency by designing new spectrally efficient pulse shapes for such digital modulations. The pulses designed are of finite duration and exhibit zero intersymbol interference when received through an additive white Gaussian noise (AWGN) channel. It is shown that the resulting communications signals have optimal spectral roll-off while maintaining optimum bit error ratio performance when received via an AWGN channel. The bandwidths and power spectral densities of communications signals using these pulses are compared with traditional spectrally efficient communications signals.

THIS PAGE INTENTIONALLY LEFT BLANK

TABLE OF CONTENTS

THIS PAGE INTENTIONALLY LEFT BLANK

LIST OF FIGURES

LIST OF TABLES

THIS PAGE INTENTIONALLY LEFT BLANK

ACKNOWLEDGMENTS

I would like to express my utmost gratitude to Professor Frank Kragh for his ever enriching encouragement and technical guidance as well as to Professor Roberto Cristi for his constructive advice, leading to the successful completion of this thesis. I would also like to thank my wife for being my efficient timekeeper, watching closely the deliverables timeline and including my “sleep time”; my 4 years old daughter for her understanding that daddy can’t be on her bedside when she sleeps.

THIS PAGE INTENTIONALLY LEFT BLANK

EXECUTIVE SUMMARY

Achieving spectral efficiency in a bandlimited environment is of utmost importance for high data rate digital communications, especially in today's Network Centric Warfare (NCW) communications architecture. NCW is an evolution from platform centric warfare to fully connected platform entities where information is shared and optimum decisions are made in a time efficient manner. This translation of informational supremacy to combat superiority critically relies on the timely and successful exchange of command and control, intelligence, surveillance, and reconnaissance information among the integrated entities in this modern battlespace. Due to the mobility military operations require, much of this communications must be done by radio. “A Picture paints a thousand words” and intelligence, surveillance, and reconnaissance is no exception. Inevitably, much of the information is imagery, video, or otherwise involves large amounts of data and thus requires high data rates for real time operations and increased situation awareness. However, the radio spectrum is in limited supply for both terrestrial and satellite communications, and consequently bandwidth is a scarce resource. In this crowded spectrum, we aim to achieve a high data rate with a small allocated channel bandwidth. Accordingly, this thesis explores a means to increase the data rate per unit bandwidth for enhanced NCW capability.

Digital modulation schemes like Phase Shift Keying (PSK) and Quadrature Amplitude (QAM) are the popular choices for such application due to their inherent bandwidth efficiency. Bandwidth efficiency, which is commonly expressed as a measure of the ratio of data rate to bandwidth occupancy of the signal, can be achieved either through increasing the number of bits per symbol or via pulse shaping. In view of the fact that the former also leads to an increase in bit error rate, this thesis explores the latter to methodologically devise new pulse shapes that are of finite time duration, exhibit zero intersymbol interference (ISI), and are optimally bandwidth efficient in terms of first null bandwidth, fractional power bandwidth, and spectral roll-off while maintaining optimum bit error ratio performance when received via an additive white Gaussian noise (AWGN) channel.

The pulses are designed by expressing an arbitrary pulse shape in terms of many unknowns, and solving for those unknowns by applying the appropriate constraints to guarantee finite duration of each pulse, zero intersymbol interference when received in an AWGN channel, and high spectral efficiency. The three main design constraints applied are periodic complex Fourier series representation of the pulse (to allow for arbitrary shape while maintaining mathematical structure), shift orthonormality condition between pulses (to ensure zero intersymbol interference), and designing the pulse with as many continuous temporal derivatives as possible (to ensure steep spectral roll-off).

This thesis has successfully shown a methodology to design finite duration pulses with first null bandwidths as well as fractional power bandwidths between half the symbol rate $(0.5/T)$ and the symbol rate $(1/T)$ and to achieve the optimum spectral roll-off for a given first null bandwidth. Additionally, these pulses exhibits zero ISI and low susceptibility to jitter. These pulses would be useful in any PSK or QAM system. The methodology is very general and can result in an infinite number of combinations of pulse durations, first null bandwidths, fractional power bandwidth, and spectral roll-offs, giving the designer a large trade space in which to trade one parameter against another to achieve design goals. Design examples with excellent combinations of first null bandwidths, fractional power bandwidth, and spectral roll-off are demonstrated herein using the pulse design methodology. Additionally, the spectral occupancy of these pulses was compared with that of root raised cosine pulses truncated to the same length with favorable results.

Since one of the design constraints is quadratic in terms of the unknowns describing the pulse shapes and since our solutions are only approximate, there is no guarantee, and indeed it is unlikely, that the solutions presented herein are unique. More work is needed to determine if simpler pulses can match the spectral desirability for the same pulse duration and the same number of unknowns. Also of interest would be investigation into the application of the additional constraint of low variation of instantaneous power, due to the effects of non-linear power amplifiers, as found in many communications systems.

I. INTRODUCTION

Achieving spectral efficiency in a bandlimited environment is of utmost importance for high data rate digital communications, especially for today's Network Centric Warfare (NCW) communications architecture. NCW is an evolution from platform centric warfare to fully connected platform entities where information is shared and optimum decisions are made in a time efficient manner. This translation of informational supremacy to combat superiority critically relies on the timely and successful exchange of command and control, intelligence, surveillance, and reconnaissance information among the integrated entities in this modern battlespace. Due to the mobility military operations require, much of this communications must be done by radio. “A Picture paints a thousand words”, and intelligence, surveillance, and reconnaissance is no exception. Inevitably, much of this information is imagery or video or otherwise involves a high volume of data and thus requires high data rates for real time operations and increased situation awareness. However the radio spectrum is in limited supply for both terrestrial and satellite communications, and consequently bandwidth is a scarce resource. In this crowded spectrum, we aim to achieve a high data rate with a small allocated channel bandwidth. Accordingly, this thesis explores a means to increase the amount of data rate per bandwidth for enhanced NCW capability.

Digital modulation schemes including Phase Shift Keying (PSK) and Quadrature Amplitude (QAM) are the popular choices for such application due to their inherent bandwidth efficiency. Bandwidth spectral efficiency is a measure of the ratio of data rate to bandwidth occupancy of the signal. The bandwidth efficiency for such schemes can be achieved either through increasing the number of bits per symbol (k) or reducing the bandwidth occupancy of the signal via pulse shaping. In view of the fact that the former also leads to an increase in bit error rate, the author explores the latter to devise new pulse shapes in a methodical manner.

A. THESIS OBJECTIVE

The objective of this research is to methodically devise new pulse shapes that are of finite duration, thus realizable, and have high spectral efficiency in terms of optimal spectral roll-off. The spectral performance of these new pulse shapes are compared to traditional pulse shapes including root raised cosine. The corresponding eye-diagram has been generated to analyze its intersymbol interference and susceptibility to jitter.

B. THESIS OUTLINE

The remaining chapters of this thesis are as follows: Chapter II discusses the fundamentals of pulse shaping in digital communications in the context of a literature review of related works. Chapter III describes the design considerations in the development of the new pulses. Chapter IV presents the spectral efficiency, intersymbol interference, and sensitivity to jitter performances of the new pulses. Chapter V presents the bandwidth efficiency of the new pulses with respect to the fractional power bandwidth. Chapter VI concludes this study and recommends focus areas for future work in this area.

II. BACKGROUND AND LITERATURE REVIEW

A bandpass communications signal is a random process. Many digital modulation schemes, including PSK and QAM, can be represented using complex envelope notation (i.e. less the carrier frequency component of communications signal) as

$$x(t) = \sum_{n=-\infty}^{\infty} D[n]\, p(t - nT) \tag{2.1}$$

where $D[n]$ is the discrete complex-valued symbol information transmitted, $p(t)$ is the complex envelope of the pulse, and T is the symbol duration. T is defined as the time interval between start of successive pulses. The radio frequency (RF) communications signal $b(t)$ in terms of the complex envelope notation is

$$b(t) = \mathrm{Re}\left\{ x(t) \exp\left(j 2\pi f_c t \right) \right\} \tag{2.2}$$

where f_c is carrier frequency.

The signal bandwidth, which is defined as the spectral occupancy of signal containing significant power, is measured from the power spectral density of the signal. If $D[n]$ is independent and identically distributed (iid), the power spectral density of $x(t)$ from [1] is

$$S_{xx}(f) = \frac{\sigma_D^2}{T} \left| P(f) \right|^2 + \frac{\mu_D^2}{T^2} \sum_{m=-\infty}^{\infty} \left| P\left(\frac{m}{T} \right) \right|^2 \delta\left(f - \frac{m}{T} \right) \tag{2.3}$$

where μ_D and σ_D^2 are the mean and variance of $D[n]$ respectively, $P(f)$ is the Fourier transform of $p(t)$, and $\delta(.)$ is the Dirac delta function. In the above equation, the second term of the right hand side represents the non-information bearing portion and this implies an inefficient use of signal power. In the usual case, μ_D is zero, and therefore Equation (2.3) reduces to

$$S_{xx}(f) = \frac{\sigma_D^2}{T} \left| P(f) \right|^2 . \tag{2.4}$$

Thus we can control the spectral characteristics of the signal $x(t)$ by controlling the spectral characteristics of the pulse $p(t)$. For a bandlimited channel of bandwidth B, we

would want to design a pulse whose spectrum is contained within the complex envelope bandwidth of $B/2$ for reduced intersymbol interference.

Phase Shift Keying (PSK) and Quadrature Amplitude Modulation (QAM) are popular modulation schemes in digital communications due to their inherent spectral efficiency. It is known from [1] that such modulation schemes' performance measures of symbol error and bit error are dependent on the energy of the pulse and are independent of the shape of the pulse, provided intersymbol interference is zero or negligible. As such, the traditional pulse shapes like rectangular pulse, root raised cosine pulse, Gaussian, and the half-sine pulse shapes are customarily used in those modulation schemes.

The rectangular pulse is of finite duration but is spectrally bandwidth inefficient. The root raised cosine and Gaussian pulse shapes are very bandwidth efficient in their infinite duration form, but they must be truncated to be realizable, thereby reducing their bandwidth efficiency. The expressions for the root raised cosine pulse in the time domain and the frequency domain are given in [2] as

$$p_{RC}(t) = \frac{(4\alpha t/T)\cos\left[\pi(1+\alpha)t/T\right] + \sin\left[\pi(1-\alpha)t/T\right]}{(\pi t/T)\left[1-(4\alpha t/T)^2\right]} \tag{2.5}$$

$$P_{RC}(f) = \begin{cases} \sqrt{T} & 0 \le |f| \le \dfrac{1-\alpha}{2T} \\ \sqrt{\dfrac{T}{2}\left[1+\cos\dfrac{\pi T}{\alpha}\left(|f|-\dfrac{1-\alpha}{2T}\right)\right]} & \dfrac{1-\alpha}{2T} < |f| \le \dfrac{1+\alpha}{2T} \\ 0 & |f| > \dfrac{1+\alpha}{2T} \end{cases} \tag{2.6}$$

where α is the roll-off factor. When truncated in time, the finite duration root raised cosine pulse in the time domain and frequency domains are

$$p'_{RC}(t) = p_{RC}(t)\,\mathrm{rect}\left(\frac{t}{T'}\right) \tag{2.7}$$

where $\mathrm{rect}\left(\dfrac{t}{T'}\right)$ is 1 when $t \in \left[-T'/2, T'/2\right]$ and 0 otherwise.

$$P_{RC}'(f) = P_{RC}(f) * T'\mathrm{sinc}(T'f). \tag{2.8}$$

Notice that the truncation in time is accompanied by a spreading out of energy in frequency as indicated by the convolution in Equation (2.8). Not surprisingly, the truncated pulses have larger bandwidth than the untruncated pulses. The bandwidth of the root raised cosine pulse is often controlled via the roll-off factor, $\alpha \in [0,1]$ with $\alpha = 0$ achieving the optimal bandwidth occupancy. When α is small, the pulse exhibits higher amplitude sidelobes and longer tails in the time domain. Henceforth, when communicating using the truncated root raised cosine pulse with small α, the output of the matched filter receiver has prominent non-zero crossing error at the integer multiples of T, leading to intersymbol interference (ISI). (See Figure 1). [2].

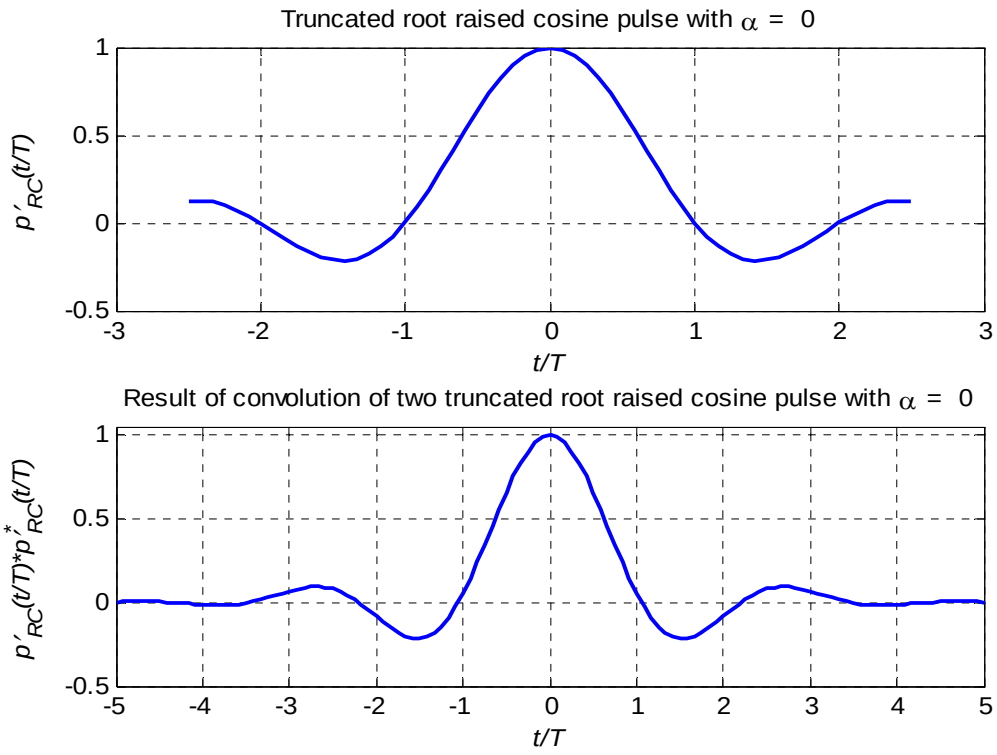

Figure 1 Nonzero crossing error due to truncation of root raised cosine pulse.

The half-sine pulse shape is more bandwidth efficient, but far from optimum. The measures of bandwidth efficiency that this thesis considers are small first null bandwidth, small fractional power bandwidth, and steep spectral roll-off.

To achieve zero ISI, the overall filter pulse response is

$$p_{overall}(t) = \frac{p(t) * p^*(-t)}{\int_{-\infty}^{\infty} |p(\tau)|^2 d\tau} \tag{2.9}$$

where $(\,)^*$ is the complex conjugate of the pulse $p(t)$. The overall filter pulse response for an optimum digital communications receiver of a complex envelope signal $x(t)$ as defined in Equation (2.1) in an AWGN channel must satisfy the first Nyquist criteria,

$$p_{overall}(nT) = \begin{cases} 1 & n = 0 \\ 0 & n \neq 0 \end{cases} \tag{2.10}$$

$p_{overall}(t)$ is known as the Nyquist pulse [1] [2]. Note that in this thesis, we are developing the new pulse $p(t)$ such that $p_{overall}(t)$ fulfills the first Nyquist criteria.

In [3], [4], [5], and [6], pulses are considered that are both bandwidth efficient and of finite duration. [3] uses an approach for continuous phase modulation that is similar to the approach used here for PSK and QAM. To achieve bandwidth efficiency and zero intersymbol interference, [3] applies the design considerations of phase shift orthogonality, and compact phase support (finite phase duration) to the phase of the modulated waveform. The treatment in [4] and [5] is ad hoc, yielding sub-optimum results. [4] determines a specific time-bandwidth product for offset QPSK type pulses that achieves a near constant signal envelope via numerical analysis. The approach in [5] achieves bandwidth efficiency by convolving a rectangular pulse with a sinusoidal frequency shift keying pulse, a variant of a minimum shift keying pulse (half-sine pulse); consequently reaping the good attributes of narrow main lobe and low power sidelobes of the rectangular pulse and sinusoidal frequency shift keying pulse respectively. [6] considers pulses of optimum bandwidth efficiency, but does not consider spectral roll-off.

Accordingly, this thesis, which closely follows the development in [7], seeks to devise a methodological approach for designing pulse shapes that are of finite time duration, exhibit zero intersymbol interference, and are optimally bandwidth efficient in terms of first null bandwidth, fractional power bandwidth, and spectral roll-off while maintaining optimum bit error ratio performance when received via an AWGN channel.

The next chapter (Chapter III) details the design considerations in the development of the new pulses.

THIS PAGE INTENTIONALLY LEFT BLANK

III. DEVELOPMENT OF NEW PULSES

The development of this chapter follows closely the development in [7].

A. PULSE DURATION

From the scaling property of the Fourier transform, it can be seen that the time domain occupancy of a signal is inversely proportional to the frequency domain occupancy of the signal [8]. From Equation (3.1), we see that scaling down the time domain occupancy of the signal $x(t)$ by a factor a, corresponds to scaling up the frequency domain occupancy of the signal by the same factor, and vice versa, where $a \neq 0$.

$$x(at) \leftrightarrow \frac{1}{|a|} X\left(\frac{f}{a}\right). \tag{3.1}$$

Henceforth, to achieve a spectrally efficient complex envelope pulse, the time duration of the pulse should be long. However, to be realizable, the pulse duration must be finite. For the development of this new pulse shape, we set the duration of the pulse to be gT, where g is chosen, for convenience, to be a positive integer and T, as defined earlier in Chapter II, is the time interval between the start of successive modulated symbols.

The finite duration pulse shape $p(t)$ can be expressed as

$$p(t) = \tilde{p}(t)\,\mathrm{rect}\left(\frac{t}{gT}\right) \tag{3.2}$$

where $\mathrm{rect}\left(\frac{t}{gT}\right)$ is 1 when $t \in [-gT/2, gT/2]$ and 0 otherwise and $\tilde{p}(t)$ can be expressed using the complex Fourier series for a periodic signal with period gT,

$$\tilde{p}(t) = \sum_{k=-\infty}^{\infty} c_k \exp\left(\frac{j2\pi kt}{gT}\right) \tag{3.3}$$

where the c_k's are the complex Fourier series coefficients of $\tilde{p}(t)$. The Fourier transform of $\tilde{p}(t)$ is

$$\tilde{P}(f) = \Im\left[\tilde{p}(t)\right]$$

$$= \Im\left[\sum_{k=-\infty}^{\infty} c_k \exp\left(\frac{j2\pi kt}{gT}\right)\right]$$

$$= \sum_{k=-\infty}^{\infty} c_k \Im\left[\exp\left(\frac{j2\pi kt}{gT}\right)\right]$$

$$= \sum_{k=-\infty}^{\infty} c_k \delta\left(f - \frac{k}{gT}\right). \tag{3.4}$$

Thus, with $\tilde{P}(f)$ being composed of impulses at integer multiples of the fundamental frequency $1/gT$ (see Figure 2), we can limit the higher harmonics of the pulse to zero to achieve a spectrally efficient pulse shape, i.e. $c_k = 0$ for all $k \notin \left[-k_{\max}, k_{\max}\right]$. Note that the Fourier series coefficients c_k are complex and are not, in general real or have the same magnitude; they are shown that way in Figure 2 just for illustration purposes. Hence, we obtain

$$\tilde{p}(t) = \sum_{k=-k_{\max}}^{k_{\max}} c_k \exp\left(\frac{j2\pi kt}{gT}\right). \tag{3.5}$$

$$\tilde{P}(f) = \sum_{k=-k_{\max}}^{k_{\max}} c_k \delta\left(f - \frac{k}{gT}\right)$$

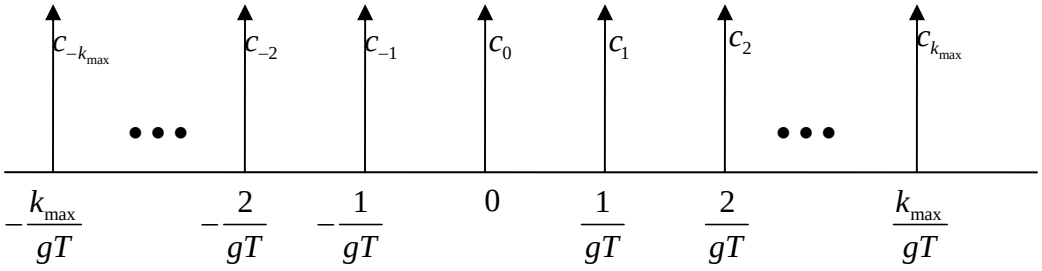

Figure 2 Fourier Transform of $\tilde{P}(f)$.

Therefore, the Fourier transform of $p(t)$ is

$$\begin{aligned} P(f) &= \Im\left[\tilde{p}(t)\,\mathrm{rect}\left(\frac{t}{gT}\right)\right] \\ &= \tilde{P}(f) * \Im\left[\mathrm{rect}\left(\frac{t}{gT}\right)\right] \\ &= \sum_{k=-k_{\max}}^{k_{\max}} c_k \delta\left(f - \frac{k}{gT}\right) * gT\,\mathrm{sinc}(gTf) \\ &= gT \sum_{k=-k_{\max}}^{k_{\max}} c_k \,\mathrm{sinc}(gTf - k). \end{aligned} \tag{3.6}$$

From the above equation, the first null occurs at $f = (k_{\max}+1)/gT$. Thus to achieve optimal spectral efficiency of the main lobe null-to-null bandwidth, $k_{\max}$ should be kept small. However, as we will see later, there are two opposing considerations to the value of $k_{\max}$; a small $k_{\max}$ will keep the width of the main lobe bandwidth small whereas a high $k_{\max}$ will yield a steep roll off of the out-of-band power spectral density.

B. ZERO INTERSYMBOL INTERFERENCE

For optimum BER performance, the impulse response of the matched filter for $p(t)$ for an optimum digital communications receiver of a complex envelope signal $x(t)$ as defined in Equation (2.1) in an AWGN channel is

$$h(t) = p^*\left(\frac{gT}{2} - t\right) \tag{3.7}$$

where $(\,)^*$ denotes the complex conjugate operation.

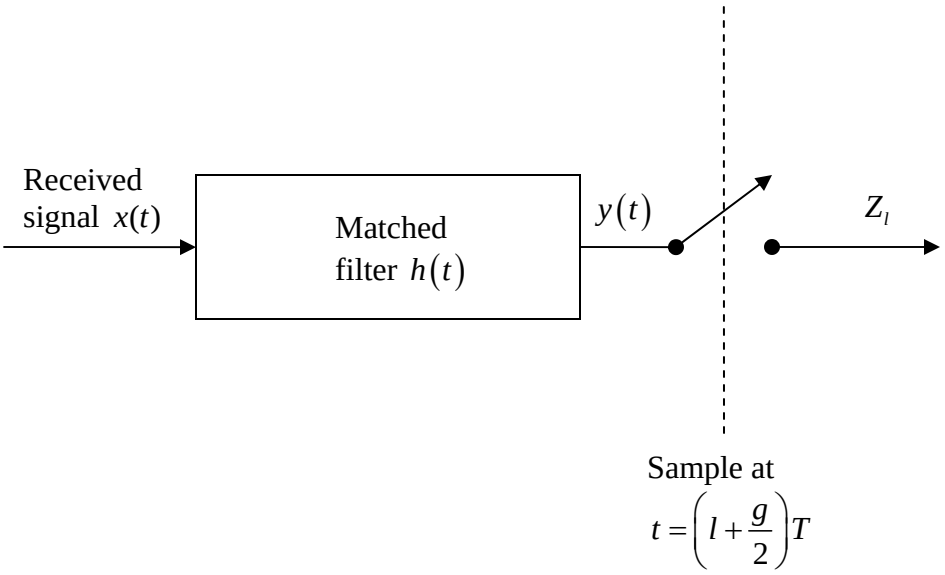

Figure 3 Matched filter receiver.

The deterministic component of the received signal at the output of the optimum receiver is

$$\begin{aligned} y(t) &= x(t) * h(t) \\ &= \int_{-\infty}^{\infty} x(\alpha) h(t-\alpha)\, d\alpha \,. \end{aligned} \tag{3.8}$$

Consequently, the noiseless decision statistic for data $D[l]$ of such an optimum receiver is

$$\begin{aligned} Z_l &= y\left(\left(l + \frac{g}{2}\right)T\right) \\ &= \int_{-\infty}^{\infty} x(\alpha) h\left(\left(l + \frac{g}{2}\right)T - \alpha\right) d\alpha \,. \end{aligned} \tag{3.9}$$

Substituting Equations (2.1) and (3.7) into (3.9) we obtain,

$$\begin{aligned} Z_l &= \int_{-\infty}^{\infty} x(\alpha) p^*\left(\frac{gT}{2} - \left[\left(l + \frac{g}{2}\right)T - \alpha\right]\right) d\alpha \\ &= \int_{-\infty}^{\infty} x(\alpha) p^*(\alpha - lT)\, d\alpha \\ &= \int_{-\infty}^{\infty} \sum_{n=-\infty}^{\infty} D[n]\, p(\alpha - nT) p^*(\alpha - lT)\, d\alpha \\ &= \sum_{n=-\infty}^{\infty} D[n] \int_{-\infty}^{\infty} p(\alpha - nT) p^*(\alpha - lT)\, d\alpha \,. \end{aligned} \tag{3.10}$$

Letting $u = \alpha - nT$, Z_l reduces to

$$Z_l = \sum_{n=-\infty}^{\infty} D[n] \int_{-\infty}^{\infty} p(u) p^*\left(u + (n-l)T\right) du \,. \tag{3.11}$$

Thus for the noiseless decision statistic Z_l to be equal to the data $D[l]$ at $\left(l + \frac{g}{2}\right)T$ sampling instances, we require

$$\int_{-\infty}^{\infty} p(u) p^*\left(u + (n-l)T\right) du = \delta_{0,n-l} \tag{3.12}$$

where δ is the Kronecker delta. As a result, we obtain,

$$Z_l = \sum_{n=-\infty}^{\infty} D[n] \delta_{0,n-l} = D[l]. \tag{3.13}$$

Henceforth from the above, we see that in order to satisfy the zero ISI condition and an arbitrary condition of unit pulse energy we can mandate the following orthonormality requirement on the pulse shape,

$$\int_{-\infty}^{\infty} p(t) p^*\left(t + nT\right) dt = \delta_{0,n} \,. \tag{3.14}$$

From [1] we know that the linear modulation schemes' performance measures of symbol error and bit error are dependent on the energy of the pulse and are independent of the shape of the pulse. Therefore we set the arbitrary condition of unit pulse energy for convenience as we want to compare pulses with identical energy that yield the same symbol error and bit error performances.

Equation (3.2) implies that $p(t)\, p^*\left(t + nT\right) = 0$ for all t whenever $|n| \geq g$. Additionally, Equation (3.14) for $-n$ is redundant with Equation (3.14) for n. Therefore, the constraints of interest from (3.14) correspond to values of $n = 0, 1, 2, \ldots, g-1$. A complex constraint can be written as two real constraints, i.e. its real and imaginary components respectively. Retrospectively, a real constraint is equivalent to one half of a complex constraint. For $n = 0$, Equation (3.14) yields one real constraint on the coefficients c_k, and for each $n = 1, 2, \ldots, g-1$, Equation (3.14) yields 2 real constraints on the coefficients c_k. Thus, Equation (3.14) yields a total of $2(g-1)+1 = 2g-1$ real constraints on the coefficients c_k. Equivalently, following the preceding argument, in terms of number of complex constraints, we also can say that Equation (3.14) yields an

effective $g-1$ distinct complex constraints and one half a complex constraint (one real constraint) on the coefficients c_k. The general expression for these constraints is derived as follows

$$\int_{-\infty}^{\infty} p(t)p^*(t+nT)\,dt = \int_{-\infty}^{\infty} \tilde{p}(t)rect\left(\frac{t}{gT}\right)\tilde{p}^*(t+nT)\,rect\left(\frac{t+nT}{gT}\right)dt$$

$$= \int_{-\frac{gT}{2}}^{\frac{gT}{2}-nT} \tilde{p}(t)\tilde{p}^*(t+nT)\,dt$$

$$= \int_{-\frac{gT}{2}}^{\frac{gT}{2}-nT} \sum_{k=-k_{\max}}^{k_{\max}} c_k \exp\left(\frac{j2\pi kt}{gT}\right) \sum_{l=-k_{\max}}^{k_{\max}} c_l^* \exp\left(\frac{-j2\pi l(t+nT)}{gT}\right)dt$$

$$= \sum_{k=-k_{\max}}^{k_{\max}} \sum_{l=-k_{\max}}^{k_{\max}} c_k c_l^* \exp\left(\frac{-j2\pi nl}{g}\right) \int_{-\frac{gT}{2}}^{\frac{gT}{2}-nT} \exp\left(\frac{j2\pi t(k-l)}{gT}\right)dt\,. \quad (3.15)$$

As an initial step to evaluate the double summation in Equation (3.15), we first consider the case when $k=l$. The contribution to the double sum in Equation (3.15) from terms where $k=l$ is

$$= (g-n)T \sum_{k=-k_{\max}}^{k_{\max}} |c_k|^2 \exp\left(\frac{-j2\pi kn}{g}\right). \quad (3.16)$$

Next, we consider the remaining terms. The contribution to the double sum in Equation (3.15) from terms where $k \neq l$ is

$$\sum_{k=-k_{\max}}^{k_{\max}} \sum_{l=-k_{\max}}^{k_{\max}} c_k c_l^{*} \exp\left(\frac{-j2\pi nl}{g}\right) \frac{gT}{j2\pi(k-l)} \exp\left(\frac{-j\pi n(k-l)}{g}\right)$$

$$\times\left[\exp\left(j\pi(k-l)\right)\exp\left(\frac{-j2\pi n(k-l)}{g}\right)-\exp\left(-j\pi(k-l)\right)\right]$$

$$= \sum_{k=-k_{\max}}^{k_{\max}} \sum_{l=-k_{\max}}^{k_{\max}} c_k c_l^{*} \exp\left(\frac{-j2\pi nl}{g}\right) \frac{gT}{j2\pi(k-l)} \exp\left(\frac{-j\pi n(k-l)}{g}\right)$$

$$\times\left[\exp\left(j\pi(k-l)\right)\exp\left(\frac{-j\pi n(k-l)}{g}\right)-\exp\left(-j\pi(k-l)\right)\exp\left(\frac{j\pi n(k-l)}{g}\right)\right]$$

$$= \sum_{k=-k_{\max}}^{k_{\max}} \sum_{l=-k_{\max}}^{k_{\max}} c_k c_l^{*} \exp\left(\frac{-j2\pi nl}{g}\right) \frac{gT}{\pi(k-l)} \exp\left(\frac{-j\pi n(k-l)}{g}\right)$$

$$\times\sin\left(\pi(k-l)-\frac{\pi n(k-l)}{g}\right)$$

$$= \sum_{k=-k_{\max}}^{k_{\max}} \sum_{l=-k_{\max}}^{k_{\max}} c_k c_l^{*} \exp\left(\frac{-j2\pi nl}{g}\right) gT\left(1-\frac{n}{g}\right) \exp\left(\frac{-j\pi n(k-l)}{g}\right)$$

$$\times\frac{\sin\left(\pi(k-l)\left(1-\frac{n}{g}\right)\right)}{\pi(k-l)\left(1-\frac{n}{g}\right)}$$

$$= \sum_{k=-k_{\max}}^{k_{\max}} \sum_{l=-k_{\max}}^{k_{\max}} c_k c_l^{*} \exp\left(\frac{-j2\pi nl}{g}\right)(g-n)T \exp\left(\frac{-j\pi n(k-l)}{g}\right)$$

$$\times\operatorname{sinc}\left((k-l)\left(1-\frac{n}{g}\right)\right)$$

$$\times\left[\exp\left(j\pi(k-l)\right)\exp\left(\frac{-j\pi n(k-l)}{g}\right)-\exp\left(-j\pi(k-l)\right)\exp\left(\frac{j\pi n(k-l)}{g}\right)\right]$$

$$= (g-n)T \sum_{k=-k_{\max}}^{k_{\max}} \sum_{l=-k_{\max}}^{k_{\max}} c_k c_l^{*} \exp\left(\frac{-j\pi n(k+l)}{g}\right) \times \operatorname{sinc}\left((k-l)\left(1-\frac{n}{g}\right)\right). \quad (3.17)$$

It is interesting to note that Equation (3.17) resolves to Equation (3.16) when setting $k = l$. Consequently, combining the preceding two cases and with Equation (3.14) we obtain

$$(g-n)T \sum_{k=-k_{\max}}^{k_{\max}} \sum_{l=-k_{\max}}^{k_{\max}} c_k c_l^{*} \exp\left(\frac{-j\pi n(k+l)}{g}\right) \times \operatorname{sinc}\left((k-l)\left(1-\frac{n}{g}\right)\right) = \delta_{0,n} \quad (3.18)$$

for $n = 0, 1, 2, \ldots, g-1$.

Specifically, the real constraint under unit energy condition in Equation (3.18) is obtained by setting $n = 0$ which yields

$$gT \sum_{k=-k_{\max}}^{k_{\max}} |c_k|^2 = 1. \quad (3.19)$$

C. SPECTRAL ROLL-OFF

We seek to design pulses that have steep spectral roll-off. From [8], the number of continuous derivatives that a function $a(t)$ possesses determines the compactness of its corresponding Fourier transform $A(f)$, or more specifically the roll-off as f increases. As an illustration, consider the frequency domain functions $\operatorname{sinc}^2(f)$ and $\operatorname{sinc}(f)$. The fact that the function $\operatorname{sinc}^2(f)$ is more compressed in its spectral occupancy and has higher spectral roll-off compared to the function $\operatorname{sinc}(f)$ can be attributed to their corresponding inverse Fourier transform functions. From Figure 4, we see that the function $rect(t) \leftrightarrow \operatorname{sinc}(f)$ has an impulsive 1st derivative in time which corresponds to a spectral roll-off of $|f|^{-1}$, or -10 decibels per decade. In contrast, the function $tri(t) \leftrightarrow \operatorname{sinc}^2(f)$ has an impulsive 2nd derivative in time with corresponding steeper spectral roll-off of $|f|^{-2}$, or -20 decibels per decade. Thus, specifically, if a function $a(t)$ is C^N (i.e. its N^{th} derivative is continuous), implying its $(N+1)^{th}$ derivative is non-

continuous and its $(N+2)^{th}$ is impulsive, then the sidelobes of $|A(f)|$ diminish at least as rapidly as $1/(f^{N+2})$, or equivalently

$$20\log_{10}|A(f)| \le K - 20(N+2)\log_{10}|f| \tag{3.20}$$

where K is an immaterial arbitrary constant in this context.

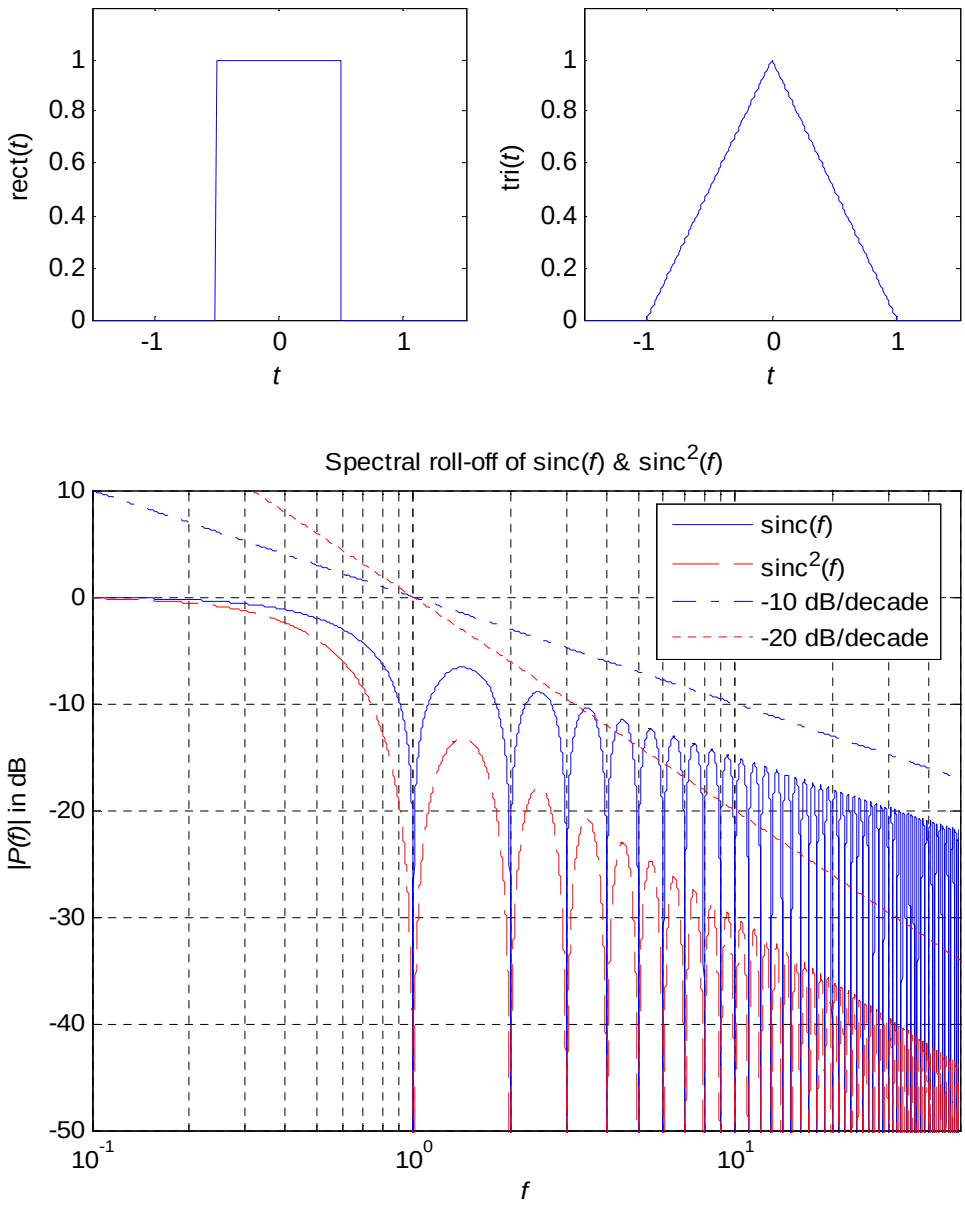

Figure 4 Comparison of spectral roll-off of $\text{sinc}(f)$ & $\text{sinc}^2(f)$.

Therefore, if our pulse shape $p(t)$ is C^N, then Equations (2.4) and (3.20) tell us that the power spectral density of our communications signal in Equation (2.1) drops off at least $20(N+2)$ decibels per decade of frequency. Hence, we desire pulses that are continuous in time and have as many continuous temporal derivatives as possible.

Therefore, we require

$$p^{(n)}\left(\pm\frac{gT}{2}\right)=0 \text{ for } n\in\{0,1,...,N\}. \tag{3.21}$$

Since $\tilde{p}(t)$ has period of gT, (3.21) yields exactly $N+1$ distinct complex constraints on the coefficients c_k. The general expression for these constraints is derived as follows:

Recall Equation (3.5), $\tilde{p}(t)=\sum_{k=-k_{\max}}^{k_{\max}} c_k \exp\left(\frac{j2\pi kt}{gT}\right)$.

Hence, by induction,

$$\tilde{p}^{(n)}(t)=\sum_{k=-k_{\max}}^{k_{\max}}\left(\frac{j2\pi k}{gT}\right)^n c_k \exp\left(\frac{j2\pi kt}{gT}\right). \tag{3.22}$$

From (3.21),

$$\begin{aligned} p^{(n)}\left(\pm\frac{gT}{2}\right) &= \tilde{p}^{(n)}\left(\pm\frac{gT}{2}\right) \\ &= \left(\frac{j2\pi}{gT}\right)^n \sum_{k=-k_{\max}}^{k_{\max}} (k)^n c_k \exp(\pm jk\pi) \\ &= \left(\frac{j2\pi}{gT}\right)^n \sum_{k=-k_{\max}}^{k_{\max}} (k)^n c_k (-1)^k = 0. \end{aligned} \tag{3.23}$$

Thus obtaining,

$$\sum_{k=-k_{\max}}^{k_{\max}} (k)^n c_k (-1)^k = 0 \text{ for } n\in\{0,1,...,N\}. \tag{3.24}$$

Equation (3.24) yields exactly $N+1$ distinct complex constraints on the coefficients c_k. Therefore, the constraints in Equations (3.18) and (3.24) constitute $g+N$ distinct complex equations and one real equation.

From the linearity Fourier transform pair, a phase rotation in the time domain of the pulse is equivalent to the same phase rotation of the pulse in frequency domain,

$$\exp(j\phi)\,p(t) \leftrightarrow \exp(j\phi)\,P(f)\,. \tag{3.25}$$

This implies that regardless of ϕ, rotation of our pulse by an arbitrary phase has no effect on the power spectral density (see Equation (2.4)). Thus, we can then arbitrarily insist that c_0 be purely real, i.e.,

$$\mathrm{Im}(c_0) = 0\,. \tag{3.26}$$

This gives one half of a complex constraint, and when combined with the constraints in Equations (3.18) and (3.24) yields an effective total of $g + N + 1$ complex constraints. Equation (3.5) indicates that there are $2k_{\max} + 1$ complex unknowns c_k. Therefore, if we choose a value for $k_{\max}$, then we can set

$$N = 2k_{\max} - g \tag{3.27}$$

to have equal numbers of constraints and unknowns. Then Equations (3.18), (3.24), and (3.26) can be solved simultaneously for the c_k coefficients, thereby determining our pulse shape via Equation (3.2).

The value of $k_{\max}$ should be chosen to achieve the desired tradeoff between first null bandwidth and spectral roll-off. Specifically, the first null of the complex lowpass equivalent signal in Equation (2.1) occurs at

$$f_1 = \frac{k_{\max} + 1}{gT} \tag{3.28}$$

and the spectral roll-off is at least

$$20(2k_{\max} - g + 2) \text{ decibels per decade of frequency}\,. \tag{3.29}$$

Therefore, small $k_{\max}$ improves the first null bandwidth while large $k_{\max}$ enhances spectral roll-off. If we insist that our pulse, $p(t)$, be continuous, then $N \geq 0$. In this case $k_{\max}$ may be chosen as small as $g/2$ which corresponds to the minimum first null $f_1 = (0.5 + 1/g)(1/T)$. Clearly, the limit of the first null bandwidth is $1/(2T)$ for very long duration pulses (i.e. large g). It is intuitively pleasing that this corresponds to the

first null bandwidth of the minimum bandwidth infinite duration pulse shape $p(t) = \text{sinc}(t/T)$, ($\leftrightarrow P(f) = T\text{rect}(fT)$). On the other hand, if we demand that our first null bandwidth be no greater than $1/T$, then, by Equation (3.28) we must insist that $k_{\max} \leq g - 1$. Typically, we will require

$$g/2 \leq k_{\max} \leq g - 1 \tag{3.30}$$

for good spectral roll off and first null bandwidth.

The above illustrations show a methodology to design fixed time duration pulses that exhibit zero intersymbol interference and steep spectral roll-off. The value of $k_{\max}$ is chosen to achieved the desired tradeoff between the null to null bandwidth and spectral roll off.

The next chapter (Chapter IV) presents the spectral efficiency, intersymbol interference, and sensitivity to jitter performances of the new pulses with varied g and $k_{\max}$ values. Equations (3.18), (3.24), and (3.26) are solved simultaneously for the c_k coefficients, thereby determining our new pulse shapes via Equation (3.2).

IV. ANALYSIS OF THE PROPOSED NEW PULSES

Adopting design considerations from Chapter III in the development of the new spectrally efficient pulse shapes, the designer should first determine the largest practical pulse duration, gT for the required communication system application. The larger this can be, the more potential there is for spectral efficiency, although there is a diminishing return as pulse duration increases. Also, the numerical computations required to solve for the coefficients c_k grows rapidly with increasing pulse duration. Next, the designer will choose $k_{\max}$ according to the desired tradeoff between the first null bandwidth and the spectral roll-off. A small $k_{\max}$ achieves a narrower null-to-null bandwidth whilst a large $k_{\max}$ achieves a steeper spectral roll-off. Then, the designer will solve for the coefficients c_k that satisfy the Equations (3.18), (3.24), and (3.26). In view of the fact that Equation (3.18) is quadratic, solving the coefficients c_k analytically is complicated except for the case of normalized duration $g = 1$. For cases of $g > 1$, numerical methods and tolerated approximate solutions via MATHCAD®'s Find Solve Block (and MATLAB®'s fsolve) are used to solve for the coefficients c_k. The following outlay of this chapter exemplifies the results achieved for varied variables g and $k_{\max}$. Additionally, the corresponding results for the root-raised cosine pulse truncated to the same duration gT are superimposed on the graphs for performance comparison purposes. For convenience, we let $T = 1$ in the numerical calculations.

A. PULSE DURATION $= T$, $k_{\max} = 1$

This is the only example in this thesis for which the solution is exact and analytically obtained as follows:

Substituting $g = 1$ into Equation (3.19) obtains,

$$\sum_{k=-1}^{1} |c_k|^2 = 1. \tag{4.1}$$

Then expanding Equation (4.1) yields

$$\left(\left|c_{-1}\right|^2+\left|c_0\right|^2+\left|c_1\right|^2\right)=1. \tag{4.2}$$

From Equation (3.27), with $g=1$ and $k_{\max}=1$, we obtained the number of continuous temporal derivatives as $N=1$. Therefore, Equation (3.24) with $n\in\{0,1\}$ yields

$$\sum_{k=-1}^{1}\left(k\right)^0 c_k\left(-1\right)^k=0 \tag{4.3}$$

which is simplified to

$$-c_{-1}+c_0-c_1=0 \tag{4.4}$$

for continuity of the pulse itself and

$$\sum_{k=-1}^{1}\left(k\right)^1 c_k\left(-1\right)^k=0 \tag{4.5}$$

which is simplified to

$$c_{-1}-c_1=0 \tag{4.6}$$

for continuity of the first derivative. Henceforth, solving Equations (3.26), (4.2), (4.4), and (4.6) simultaneously yields the coefficients c_k as shown in Table 1 below.

Table 1 Coefficients c_k for new pulse of duration T with $k_{\max}=1$.

c_{-1}	$1/\sqrt{6}$
c_0	$2/\sqrt{6}$
c_1	$1/\sqrt{6}$

Substituting this result into Equations (3.2) and (3.6) yields $p(t)$ and $\left|P\left(f\right)\right|^2$, which are as shown in Figure 5. The root-raised cosine pulse truncated to the same duration T in Equations (2.7) and (2.8) yields $p'_{RC}\left(t\right)$ and $\left|P'_{RC}\left(f\right)\right|^2$ which are superimposed on the graph for performance comparison. Note in this case, the first null bandwidth of the truncated root-raised cosine is smaller than the first null bandwidth of the new pulse. However, the spectral roll-off of the new pulse is much better than that of the truncated root-raised cosine pulse. This example is for illustrative purposes only, as the short duration of the pulse greatly limits its spectral efficiency.

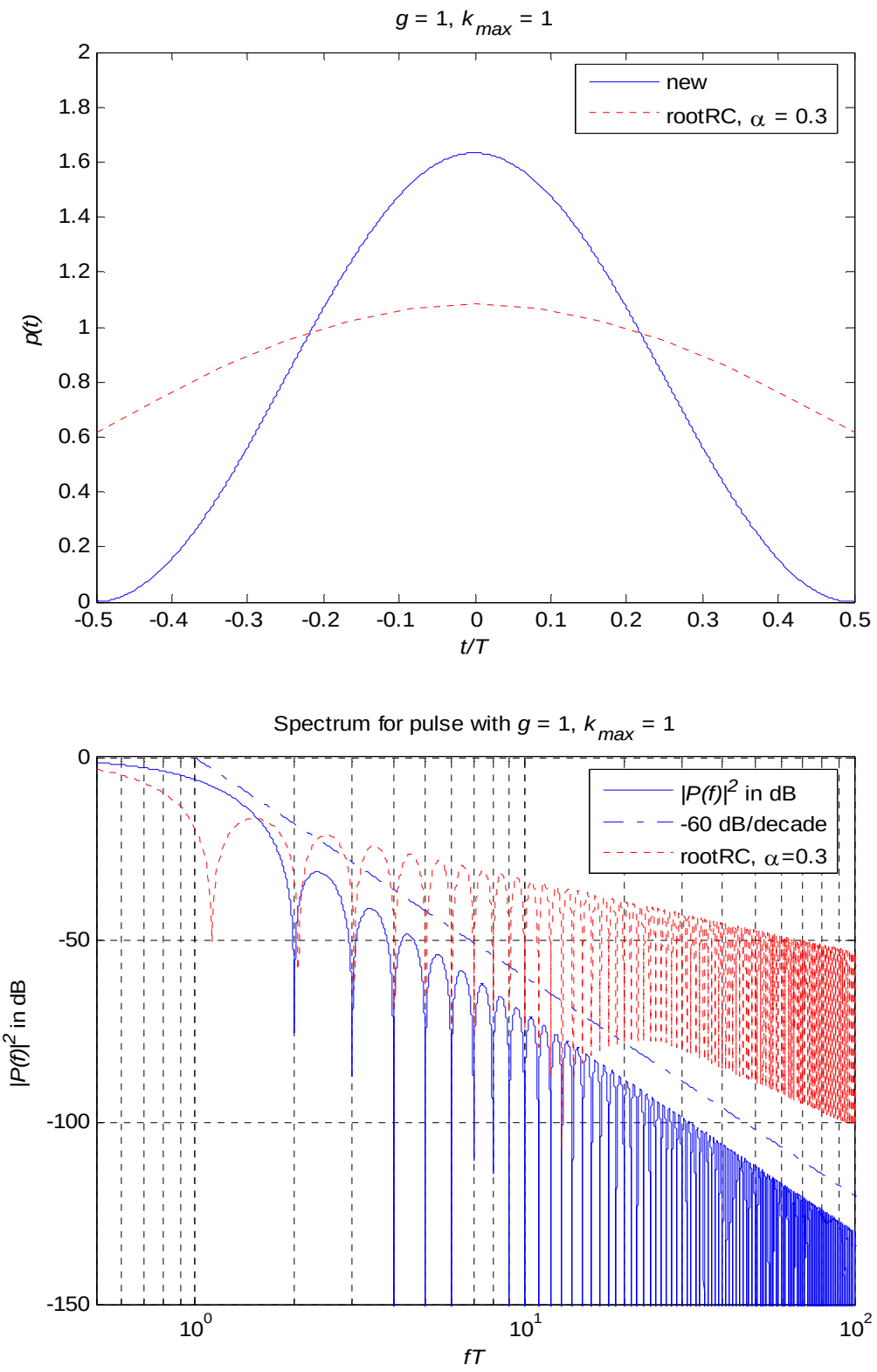

Figure 5 Comparison of duration T, new (with $k_{\max} = 1$) and truncated root raised cosine (with $\alpha = 0.3$) pulse shapes.

B. PULSE DURATION $= 5T$, $k_{max} = 5$

In this section we design a longer duration pulse with the hopes of increased spectral efficiency, choosing $g = 5$ as a compromise between spectral efficiency and computational complexity. $k_{max} = 5$ is a large value and is chosen to illustrate sharp spectral roll off.

The simultaneous solution of Equations (3.18), (3.24), and (3.26) yields the coefficients c_k as shown in Table 2 below,

Table 2 Coefficients c_k for new pulse of duration $5T$ with $k_{max} = 5$.

c_{-5}	$3.6372 \times 10^{-3} + j7.9971 \times 10^{-3}$
c_{-4}	$0.0268 + j0.0408$
c_{-3}	$0.0851 + j0.0829$
c_{-2}	$0.1555 + j0.0822$
c_{-1}	$0.1937 + j0.0361$
c_0	0.1997
c_1	$0.1939 + j1.9040 \times 10^{-3}$
c_2	$0.1595 + j0.0216$
c_3	$0.0908 + j0.0286$
c_4	$0.0300 + j0.0164$
c_5	$4.2697 \times 10^{-3} + j3.5962 \times 10^{-3}$

Substituting this result into Equations (3.2) and (3.6) yields $p(t)$ and $\left|P\left(f\right)\right|^2$, which are as shown in Figure 6. The root-raised cosine pulse truncated to the same duration $5T$ in Equations (2.7) and (2.8) yields $p'_{RC}\left(t\right)$ and $\left|P'_{RC}\left(f\right)\right|^2$ which are superimposed on the graph for performance comparison. In this case we see that by increasing the duration of the new pulse from the previous example of T to $5T$ we achieve a smaller first null bandwidth. The first null bandwidth is $1.2/T$ as predicted by Equation (3.28) and the spectral roll-off is -140 dB/decade as predicted by Equation (3.29). This first null bandwidth of the new pulse is larger than the first null bandwidth of the truncated root-raised cosine. However, the spectral roll-off of this new pulse is substantially better than that of the truncated root-raised cosine pulse.

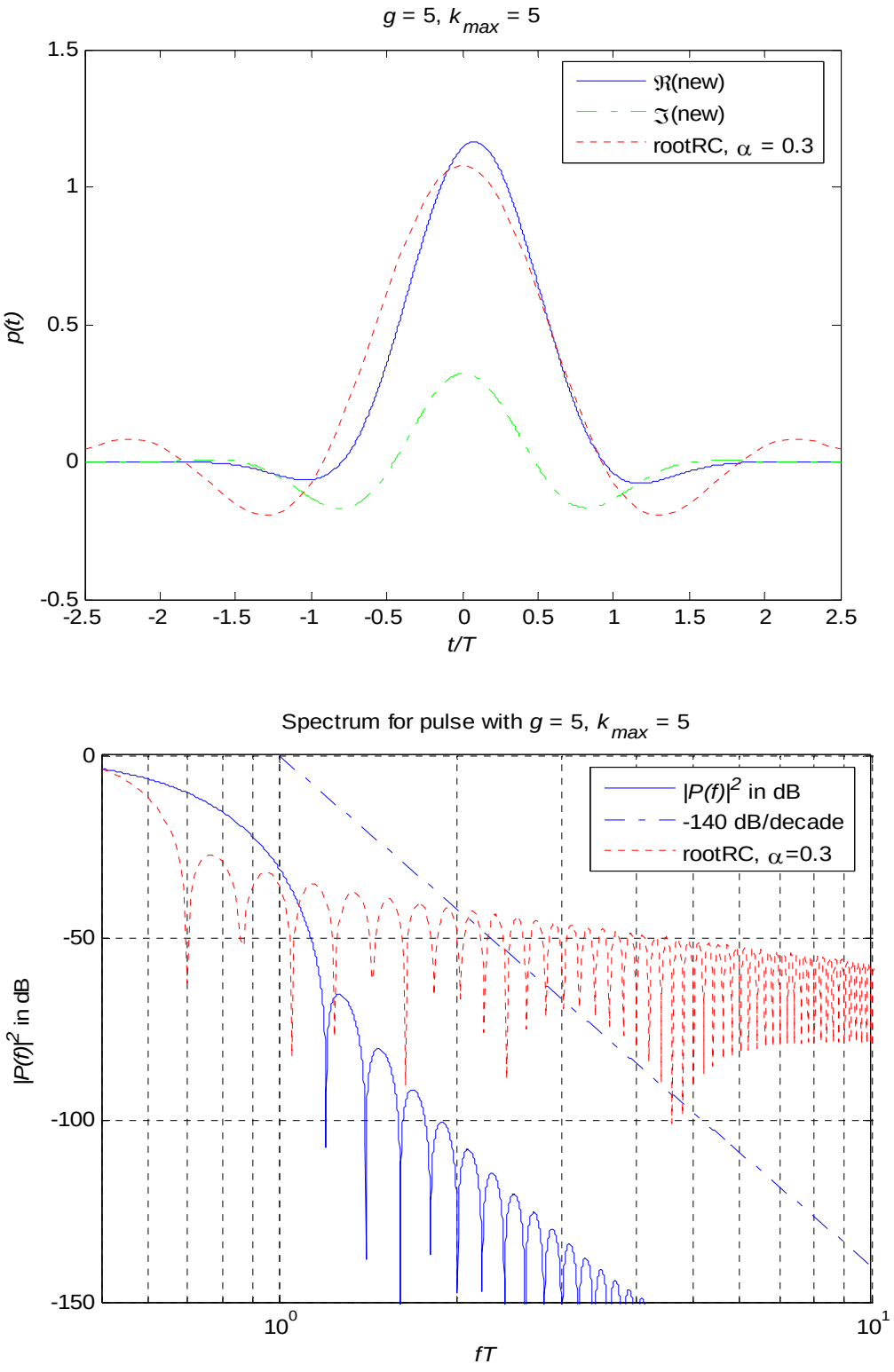

Figure 6 Comparison of duration $5T$, new (with $k_{\max} = 5$) and truncated root raised cosine (with $\alpha = 0.3$) pulse shapes.

C. PULSE DURATION $= 5T$, $k_{max} = 4$

In this section we design a pulse equal in duration to the prior pulse with a reduction in k_{max} of one, to illustrate how this improves first null bandwidth at the expense of decreased spectral roll off.

The simultaneous solution of Equations (3.18), (3.24), and (3.26) yields the coefficients c_k as shown in Table 3 below,

Table 3 Coefficients c_k for new pulse of duration $5T$ with $k_{max} = 4$.

c_{-4}	$-0.0180 + j0.0181$
c_{-3}	$-0.0981 + j0.0191$
c_{-2}	$-0.1382 - j0.1044$
c_{-1}	$0.0419 - j0.1939$
c_0	0.2000
c_1	$0.0419 + j0.1939$
c_2	$-0.1382 + j0.1044$
c_3	$-0.0981 - j0.0191$
c_4	$-0.0180 - j0.0181$

Substituting this result into Equations (3.2) and (3.6) yields $p(t)$ and $\left|P\left(f\right)\right|^2$, which are as shown in Figure 7. The root-raised cosine pulse truncated to the same duration $5T$ in Equations (2.7) and (2.8) yields $p'_{RC}\left(t\right)$ and $\left|P'_{RC}\left(f\right)\right|^2$ which are superimposed on the graph for performance comparison. Note, in this case that the first null bandwidth is $1/T$ as predicted by Equation (3.28) and the spectral roll-off is -100 dB/decade as predicted by Equation (3.29). In contrast to the pulse in Figure 6, this is a good example illustrating that by reducing $k_{\max}$ from 5 to 4, we are sacrificing spectral roll-off for improved first null bandwidth performance. This first null bandwidth of the new pulse is still larger than the first null bandwidth of the truncated root-raised cosine. However, the spectral roll-off of this new pulse is still substantially better than that of the truncated root-raised cosine pulse even with the trade off between spectral roll-off for improved first null bandwidth performance. This example demonstrates that for equal duration new pulses, we can control the $k_{\max}$ to yield the required first null bandwidth and spectral roll-off. Additionally we see that by setting $k_{\max} \le g-1$ we can achieve first null bandwidth less than or equal to$1/T$.

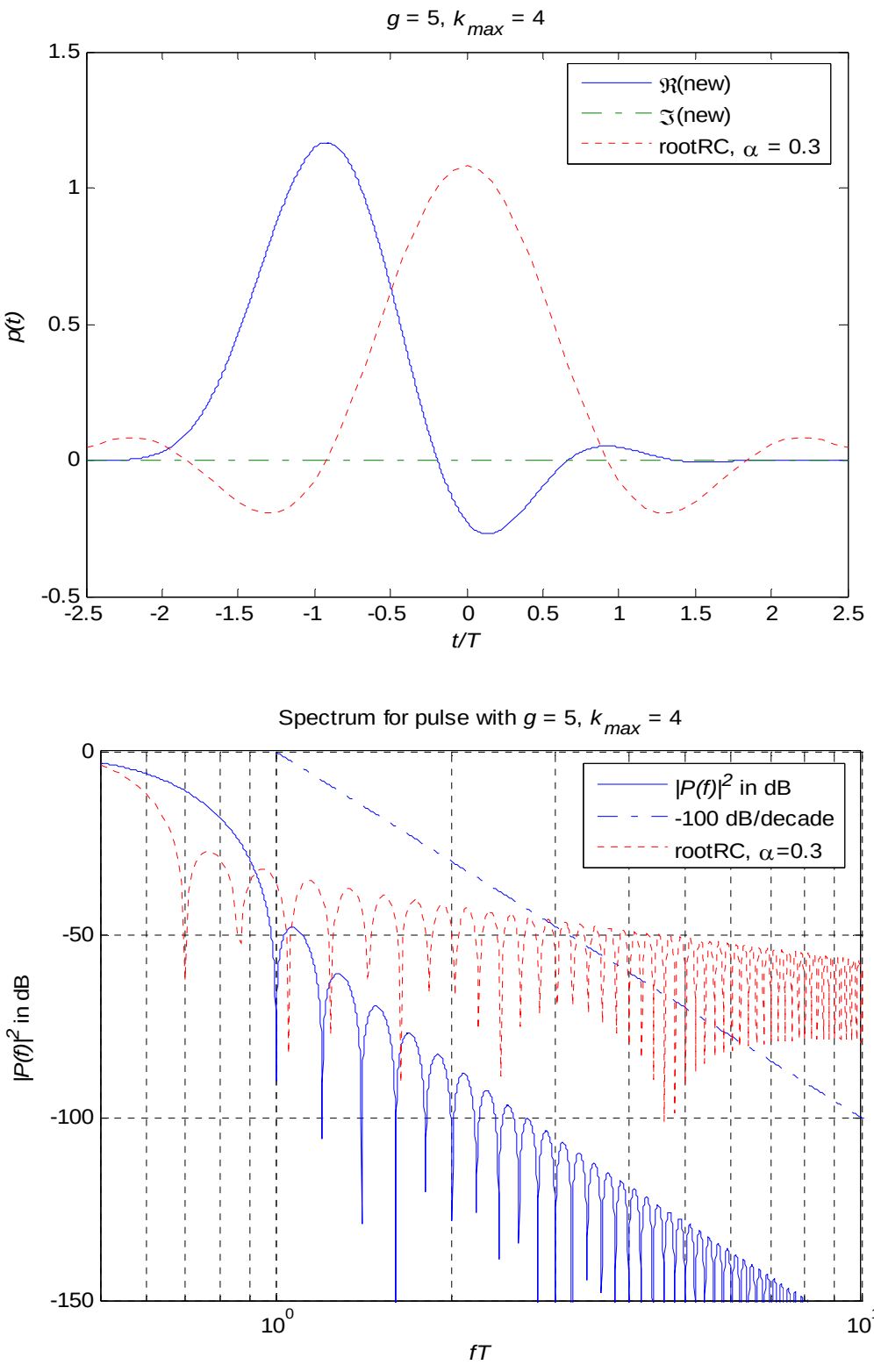

Figure 7 Comparison of duration $5T$, new (with $k_{\max} = 4$) and truncated root raised cosine (with $\alpha = 0.3$) pulse shapes.

D. PULSE DURATION = 8*T* , $k_{max} = 5$

In this section we design an even longer duration pulse with the hopes of increased spectral efficiency, choosing $g = 8$ as the design with greatest computational complexity attempted as part of this work. Our guidance in Equation (3.30) suggests constraining k_{max} such that $4 \le k_{max} \le 7$, so we choose a value from the middle of the range as a value that should yield both good spectral roll off and good first null bandwidth.

The simultaneous solution of Equations (3.18), (3.24), and (3.26) yields the coefficients c_k as shown in Table 4 below,

Table 4 Coefficients c_k for new pulse of duration $8T$ with $k_{max} = 5$.

c_{-5}	$0.0212 - j0.0018$
c_{-4}	$0.0724 + j0.0339$
c_{-3}	$0.0259 + j0.1175$
c_{-2}	$-0.1162 + j0.0460$
c_{-1}	$-0.0303 - j0.1213$
c_0	0.1250
c_1	$-0.0336 + j0.1204$
c_2	$-0.1100 - j0.0593$
c_3	$0.0625 - j0.1062$
c_4	$0.0949 + j0.0150$
c_5	$0.0204 + j0.0269$

Substituting this result into Equations (3.2) and (3.6) yields $p(t)$ and $\left|P\left(f\right)\right|^2$, which are as shown in Figure 8. The root-raised cosine pulse truncated to the same duration $8T$ in Equations (2.7) and (2.8) yields $p'_{RC}\left(t\right)$ and $\left|P'_{RC}\left(f\right)\right|^2$ which are superimposed on the graph for performance comparison. Note, in this case that the first null bandwidth is $0.75/T$ as predicted by Equation (3.28) and the spectral roll-off is -80 dB/decade as predicted by Equation (3.29). This first null bandwidth of the new pulse is larger than the first null bandwidth of the truncated root-raised cosine. However, the spectral roll-off of this new pulse is substantially better than that of the truncated root-raised cosine pulse. This is a good example of fairly even balance in the first null bandwidth versus spectral roll-off tradeoff.

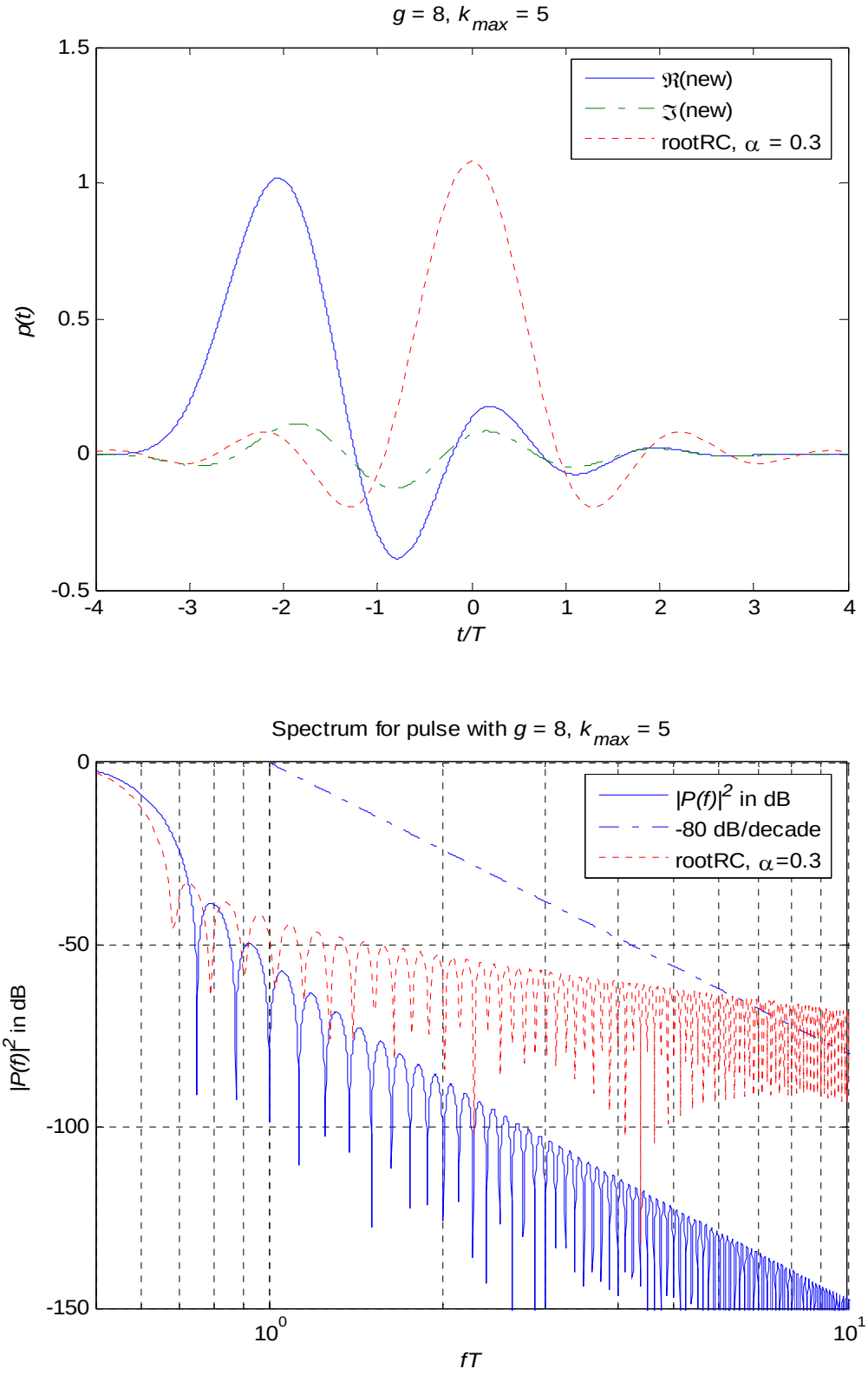

Figure 8 Comparison of duration $8T$, new (with $k_{\max} = 5$) and truncated root raised cosine (with $\alpha = 0.3$) pulse shapes.

E. PULSE DURATION = $8T$, $k_{max} = 4$

In this section we design a pulse equal in duration to the prior pulse, but this time we use the minimum k_{max} consistent with our guidance in Equation (3.30) to illustrate improved first null bandwidth at the expense of decreased spectral roll off.

The simultaneous solution of Equations (3.18), (3.24), and (3.26) yields the coefficients c_k as shown in Table 5 below,

Table 5 Coefficients c_k for new pulse of duration $8T$ with $k_{max} = 4$.

c_{-4}	$0.0864 + j0.0187$
c_{-3}	$0.1218 - j0.0280$
c_{-2}	$0.1104 - j0.0587$
c_{-1}	$0.1236 - j0.0188$
c_0	0.1250
c_1	$0.1210 - j0.0313$
c_2	$0.1126 - j0.0542$
c_3	$0.0685 - j0.1045$
c_4	$5.5627 \times 10^{-4} - j0.0884$

Substituting this result into Equations (3.2) and (3.6) yields $p(t)$ and $\left|P\left(f\right)\right|^2$, which are as shown in Figure 9. Note, in this case that the first null bandwidth is $0.625/T$ as predicted by Equation (3.28) and the spectral roll-off is -40 dB/decade as predicted by Equation (3.29). In contrast to the pulse in Figure 8, this example illustrates that by sacrificing the spectral roll-off of this pulse to itself being continuous, implying its second derivative is impulsive, the pulse has smaller first null bandwidth compared to the truncated root-raised cosine pulse. The spectral roll-off of the new pulse also outperforms the truncated root raised cosine, from frequency of $3/T$ onwards. Thus this new pulse is more spectrally efficient that the truncated root raised cosine pulse in both measures of spectral efficiency employed here, namely first null bandwidth and spectral roll-off.

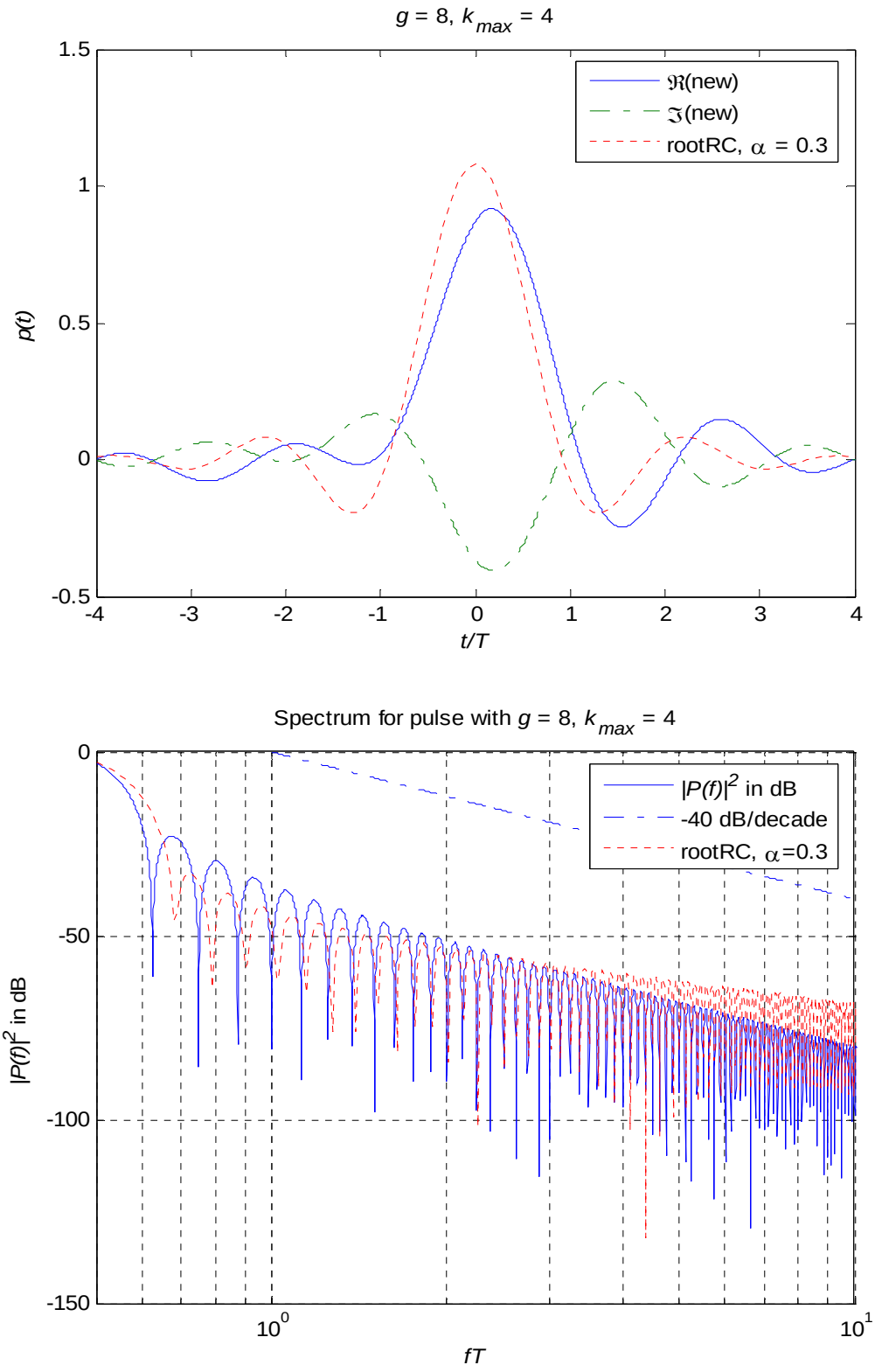

Figure 9 Comparison of duration $8T$, new (with $k_{\max} = 4$) and truncated root raised cosine (with $\alpha = 0.3$) pulse shapes.

F. PULSE INTERSYMBOL INTERFERENCE PERFORMANCE

Intersymbol interference (ISI) and sensitivity to jitter are analyzed heuristically by examining the eye diagram, which is essentially a plot of the matched filter output as a function of time for all possible data sequences superimposed upon one another. Specifically, the superposition of every snapshot of a $2T$ interval of the matched filter output using Equation (2.9) with binary antipodal modulation (i.e. $D[n] = \pm 1$) yields the eye diagram. The eye diagram provides visible evidence of compliance or non compliance with the first Nyquist criterion (see Equation (2.10)). A compliant waveform will exactly take on the values of ± 1 at the vertical axis when time t is an integer multiple of T, indicating zero ISI. This compliant waveform is called a Nyquist pulse. The $p(t) = \text{sinc}(t/T)$ pulse has ideal spectral properties, but is not used, even in truncated form, in practical systems due its sensitivity to jitter. The well-known root raised cosine pulse with raised cosine waveform at the output of the matched filter is compared against the new pulses at their matched filter outputs for relative comparisons of sensitivity to ISI and jitter. The below table shows the parameters of the new pulses that are used in this section. Note that x^T implies the transpose of x.

Table 6 New pulses' coefficients c_k for ISI analysis.

New pulse with duration $2T$ and $k_{\max} = 2$	$(c_{-2}, c_{-1}, \ldots c_2) = \begin{pmatrix} 0.0791 + j0.0791 \\ 0.3162 + j0.1581 \\ 0.4743 \\ 0.3162 - j0.1581 \\ 0.0791 - j0.0791 \end{pmatrix}^T$
New pulse with duration $3T$ and $k_{\max} = 3$	$(c_{-3}, c_{-2}, \ldots c_3) = \begin{pmatrix} 0.0371 - j0.0144 \\ 0.1538 - j0.0578 \\ 0.2809 - j0.0722 \\ 0.3285 \\ 0.2809 + j0.0722 \\ 0.1538 + j0.0578 \\ 0.0371 + j0.0144 \end{pmatrix}^T$
New pulse with duration $4T$ and $k_{\max} = 4$	$(c_{-4}, c_{-3}, \ldots c_4) = \begin{pmatrix} 8.7515 \times 10^{-4} - j0.0157 \\ 0.0163 - j0.0785 \\ 0.0807 - j0.157 \\ 0.1897 - j0.1416 \\ 0.2490 \\ 0.1896 + j0.1418 \\ 0.0804 + j0.1575 \\ 0.0160 + j0.0787 \\ 7.8554 \times 10^{-4} + j0.0157 \end{pmatrix}^T$
New pulse with duration $5T$ and $k_{\max} = 5$	See Section B of this chapter for the coefficients c_k of this pulse

From Equation (2.9), the waveforms generated using the new pulse with duration $5T$ and $k_{\max} = 5$ (see Table 6 for the respective coefficients c_k), and the root raised cosine truncated to the same duration at the respective receivers' matched filters' outputs

are as shown in Figure 10. In this time domain plot, we see that the raised cosine waveform at the matched filter output has higher and longer tails as compared to the new Nyquist waveform at the matched filter output. Additionally, the raised cosine waveform shows significant zero crossing errors at the integer multiples of T. This is due to the truncation of the root raised cosine pulse. Consequently, these results indicate that the new pulse should outperform the root raised cosine pulse in terms of insensitivity to ISI and jitter, as is illustrated in their respective eye diagrams.

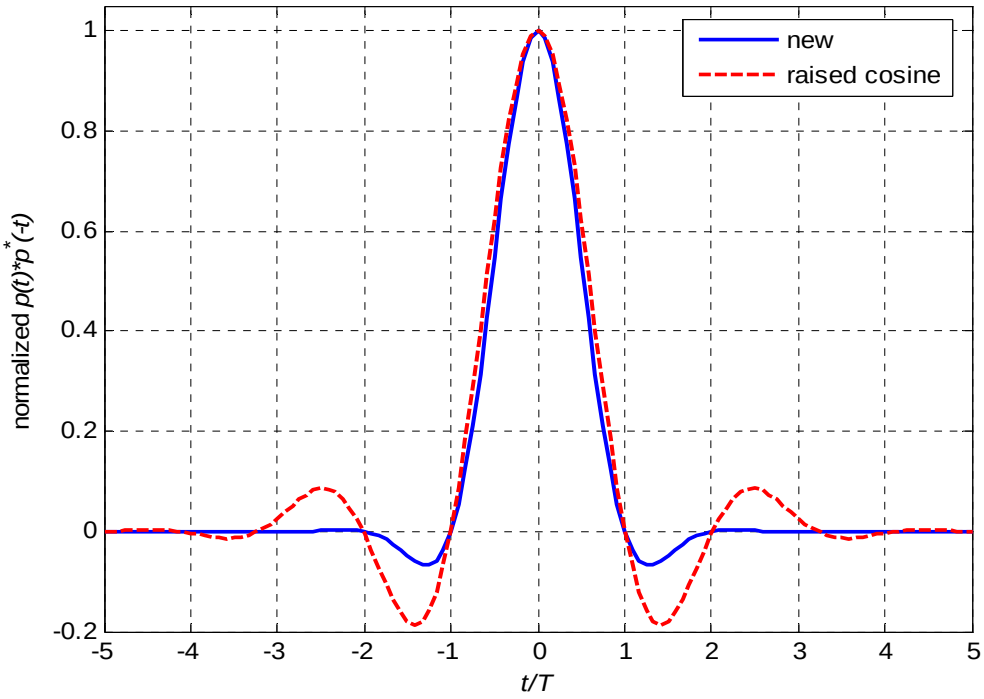

Figure 10 Comparison of matched filter outputs for systems using duration $5T$, new (with $k_{\max} = 5$) and truncated root raised cosine (with $\alpha = 0.3$) pulses.

Figure 11 and Figure 12 show the respective eye diagrams of these waveforms. The vertical opening of the eye measures the lack of ISI whereas the horizontal opening of the eye measures the insensitivity to jitter. In Figure 11, we see that the new pulse achieves zero ISI as its normalized eye pattern takes on the values of exactly ± 1 at the vertical axis when time t is an integer multiple of T. In contrast, as predicted, the truncated root raised cosine has ISI (i.e. not a value of ± 1 at the vertical axis) when t is

an integer multiple of T. Additionally, the root raised cosine has smaller horizontal eye pattern opening compared to the new pulse as a result of its higher amplitude and longer tails.

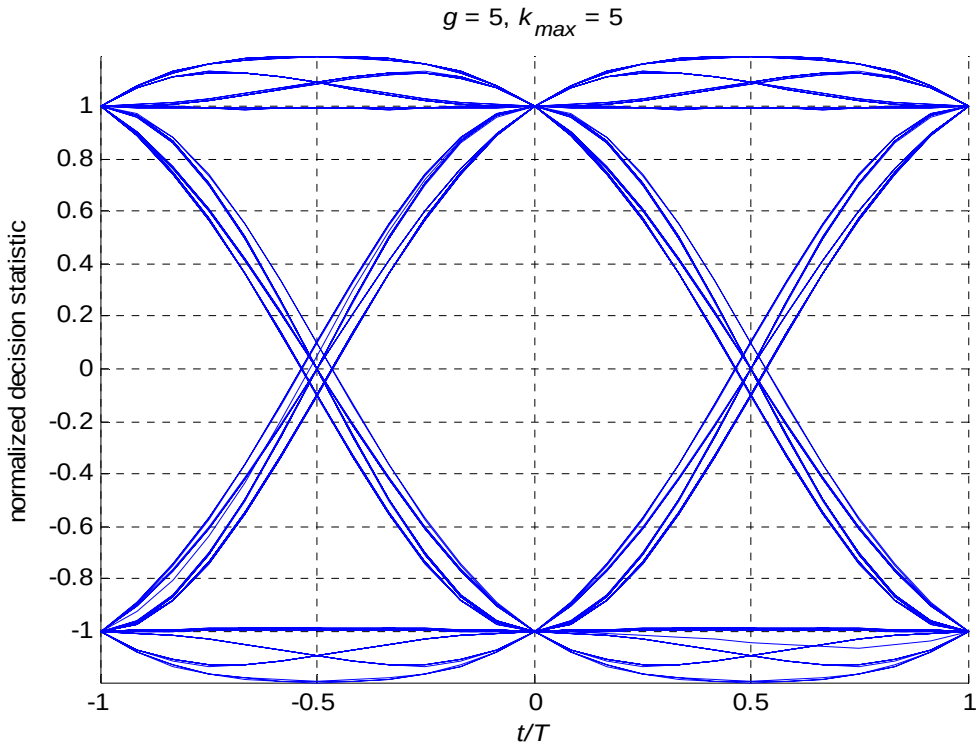

Figure 11 Eye diagram of waveform at matched filter output for system using the new pulse with duration $5T$.

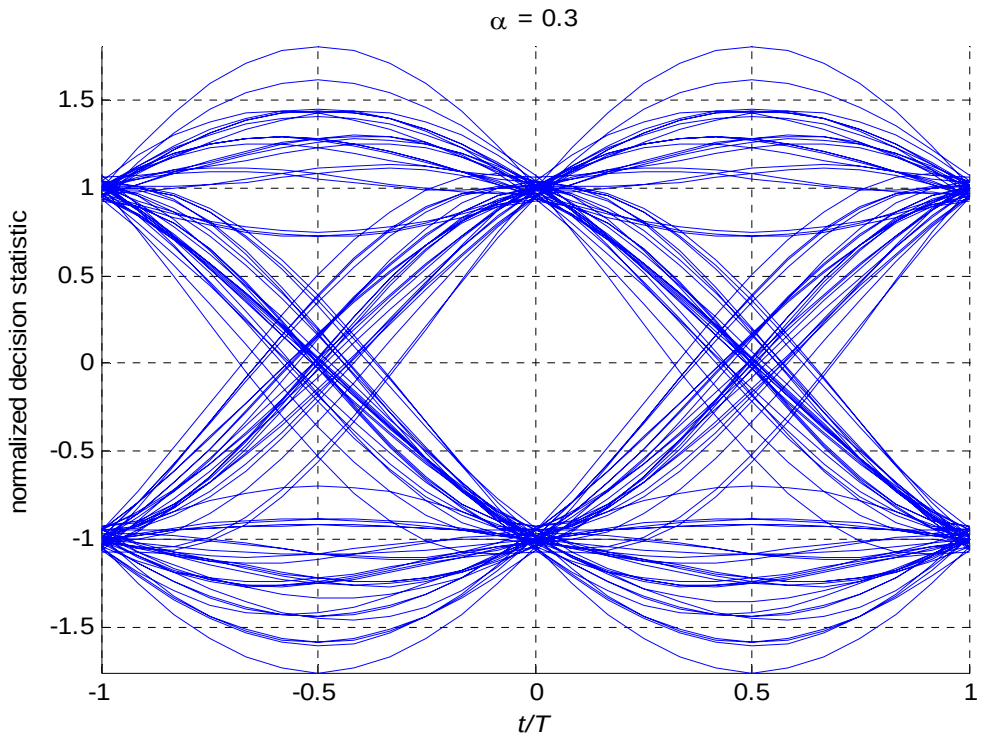

Figure 12 Eye diagram of waveform at the matched filter output for system using truncated root raised cosine pulse..

From the perspective of analyzing the new pulses with increasing pulse duration, the new pulses of duration $2T$ with $k_{\max} = 2$, duration $3T$ with $k_{\max} = 3$, duration $4T$ with $k_{\max} = 4$, and duration $5T$ with $k_{\max} = 3$ (see Table 6 for the respective coefficients c_k) are used in this analysis. As can be seen in Figure 13, the tails of the waveforms at the output of matched filter increase as pulse duration increases while maintaining the zero crossing when time t is an integer multiple of T. These increasing tails should have minimal impact in terms of sensitivity to jitter performance since as shown in the eye diagrams of the respective pulse duration (see Figure 11, Figure 14, Figure 15, and Figure 16) the horizontal openings are still within $\pm 0.3T$. The susceptibility to jitter of this new pulse should be low. Additionally, based on the eye diagrams, the pulses have good noise margin and is unlikely to cause decision errors without excessive noise.

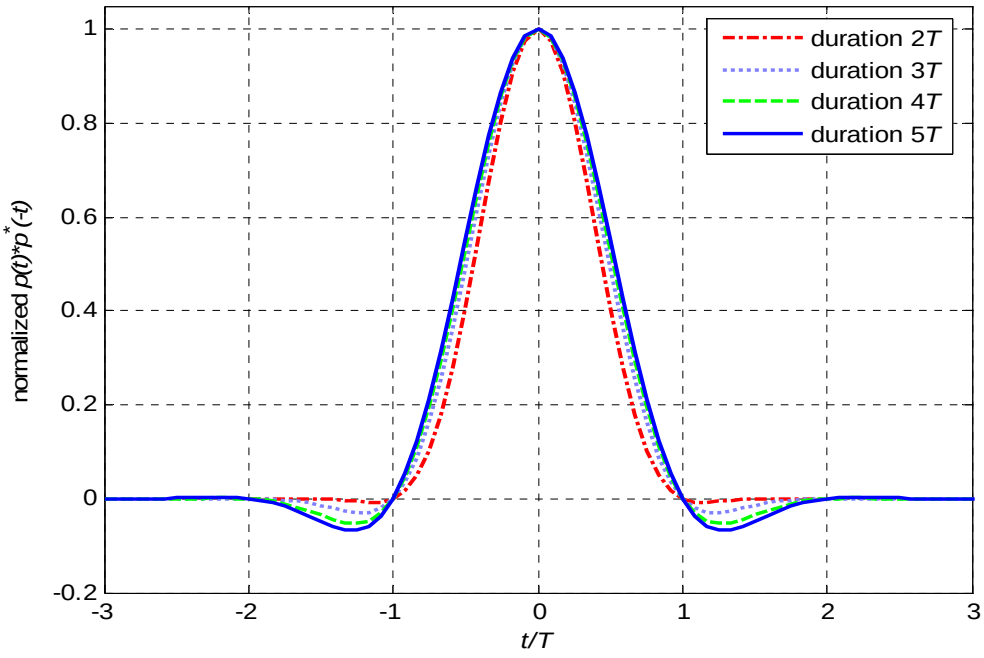

Figure 13 Comparison of waveforms at the matched filter output for systems using the new pulses with varied pulse durations.

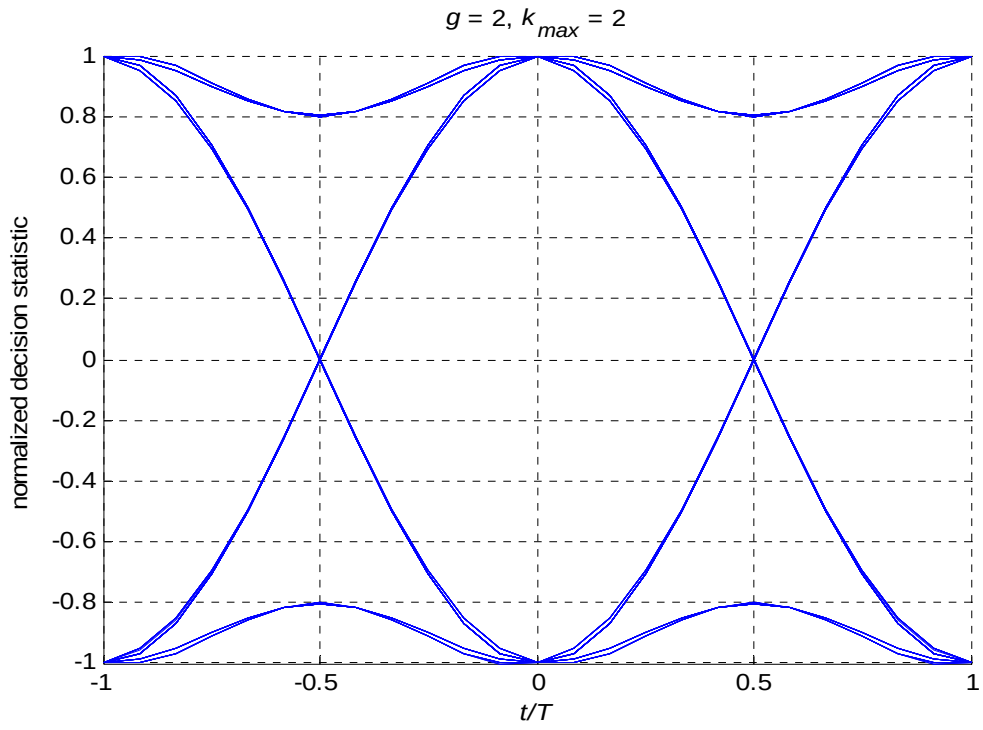

Figure 14 Eye diagram of waveform at the matched filter output for system using the new pulse with duration $2T$.

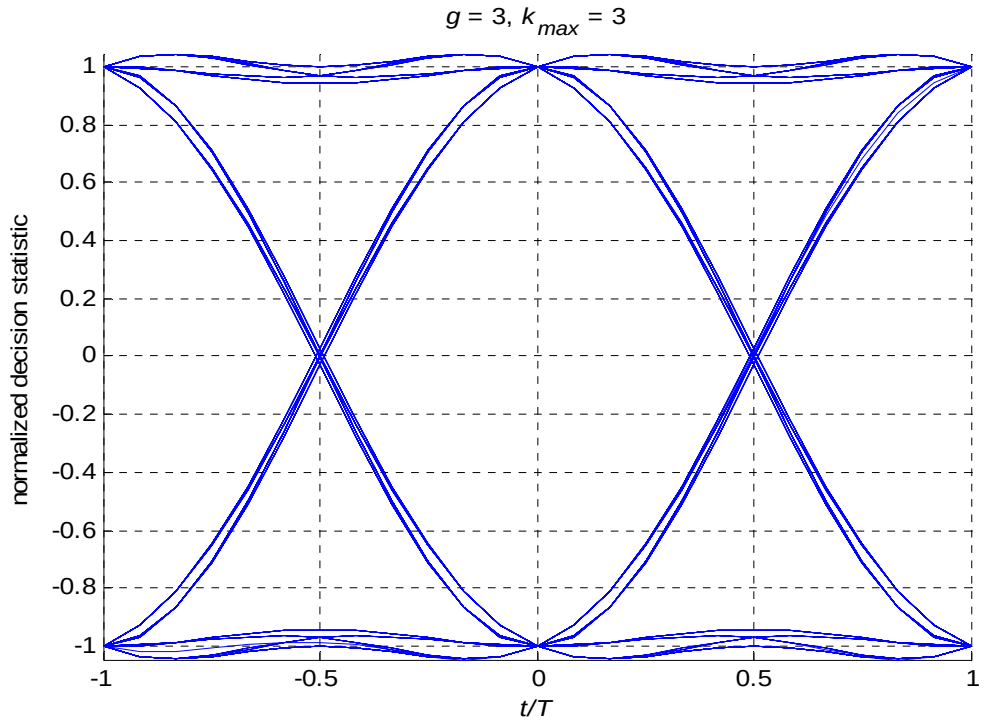

Figure 15 Eye diagram of waveform at the matched filter output for system using the new pulse with duration $3T$.

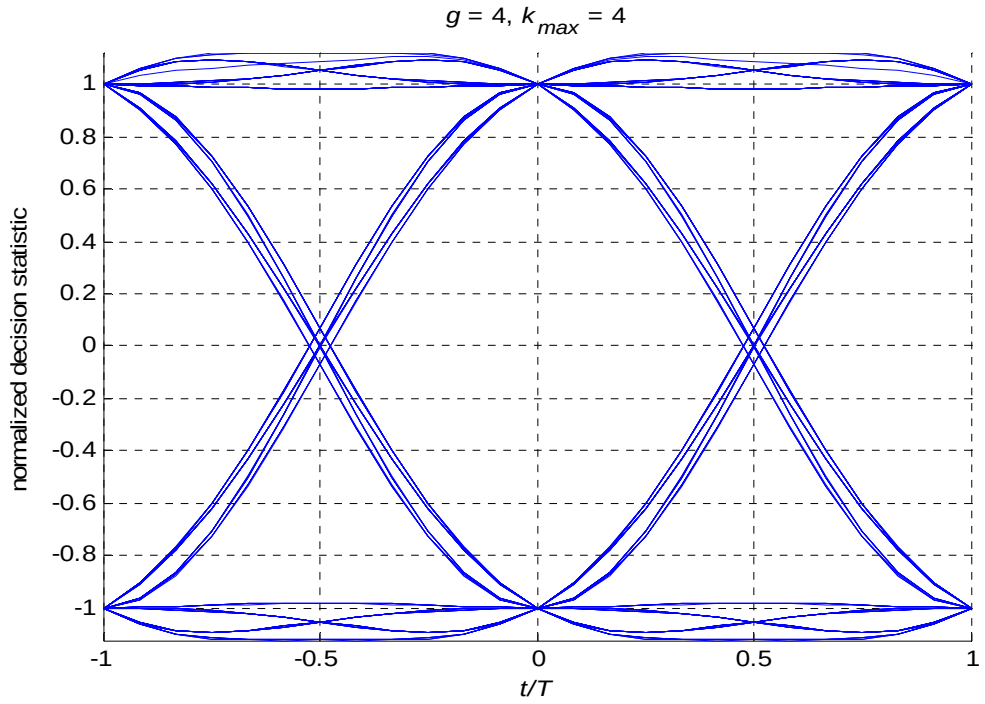

Figure 16 Eye diagram of waveform at the matched filter output for system using the new pulse with duration $4T$.

From the above illustrations in this chapter, there are indeed many permutations and combinations of g and $k_{\max}$ available to devise an appropriate pulse for a required digital communications system. As the duration of the pulse, gT, is increased, the possibilities for increased spectral efficiency improved further. For example, for $g = 20$, using our guidance in Equation (3.30) $k_{\max}$ can be as small as 10, corresponding to a first null bandwidth of $0.55/T$ and a spectral roll-off of -40 dB/decade or $k_{\max}$ can be as large as 19, yielding a first null bandwidth of $1/T$ and a spectral roll-off of -400 dB/decade. A representative compromise value of $k_{\max} = 14$ yields a first null bandwidth of $0.75/T$ and a spectral roll-off of -200 dB/decade. The eye diagrams revealed that the pulses exhibit zero intersymbol interference and favorable robustness to jitter.

The next chapter (Chapter V) demonstrates the bandwidth efficiency of the new pulses with respect to its fractional power bandwidth.

V. FRACTIONAL POWER BANDWIDTH

Fractional power bandwidth is a measure of the bandwidth that contains a specified percentage of the overall power of a signal. Specifically, a 0.99 power bandwidth implies 99% of the signal power is contained in the 99% power bandwidth w, leaving 0.5% power at both the upper and lower limit outside this bandwidth. This 0.99 power bandwidth criterion is adopted by the Federal Communications Commission (FCC) as a yardstick for signal power bandwidth control. This chapter seeks to investigate the fractional power bandwidth containment possible by designing new pulses at different g and $k_{\max}$ values based on the required digital communications application by adding an additional power bandwidth consideration to the pulse development illustrated in Chapter III. This new constraint does not optimize the power bandwidth; it calculates the power bandwidth w for the new pulse that satisfies all the applied design constraints.

Using the arbitrary condition of unit pulse energy of the shift orthonormality requirement on the new pulse shapes (when $n = 0$) from Equation (3.14), the following expressions are derived for the calculation of the fractional power bandwidth containment of this pulse starting with the unit energy condition

$$\int_{-\infty}^{\infty} \left| p(t) \right|^2 dt = 1 . \tag{5.1}$$

Using Parseval's theorem and Equation (5.1) yields

$$\int_{-\infty}^{\infty} \left| P(f) \right|^2 df = 1 \tag{5.2}$$

where recalling from Equation (3.6), $P(f) = gT \sum_{k=-k_{\max}}^{k_{\max}} c_k \operatorname{sinc}(gTf - k)$.

Thus, from Equation (5.2), the power of the signal $x(t)$ as defined in Equation (2.1) is

$$\frac{1}{T} \int_{-\infty}^{\infty} \left| P(f) \right|^2 df = \frac{1}{T} \tag{5.3}$$

where the data process, $D[n]$, is assumed to have unit variance.

Therefore, the fractional power Y of this pulse at bandwidth w is

$$\frac{1}{T}\int_{-w}^{w}\left|P(f)\right|^2 df = \frac{Y}{T}$$

$$\int_{-w}^{w}\left|gT\sum_{k=-k_{\max}}^{k_{\max}} c_k \operatorname{sinc}(gTf-k)\right|^2 df = Y\,. \tag{5.4}$$

This fractional power bandwidth design constraint yields one real equation. Thus, with the constraints from Equations (3.18), (3.24), and (3.26), there are now an effective of $g+N+1$ distinct complex equations and one real equation. To design a spectrally efficient pulse shape consistent with Chapter III pulse development, we again choose a value for $k_{\max}$ to achieve the desired tradeoff between null to null bandwidth and spectral roll off, then set the number of continuous temporal derivatives of the pulse to $N = 2k_{\max} - g$. Subsequently, Equations (3.18), (3.24), (3.26), and (5.4)can be solved simultaneously for the c_k coefficients and the fractional power bandwidth w based on the equal numbers of constraints and unknowns, thereby determining our pulse shape via Equation (3.2) that fulfill the fractional power bandwidth containment requirement.

Below are illustrative examples of coefficients c_k and fractional power bandwidth w for varied variables g and $k_{\max}$ with fractional power $Y = 0.99$ calculated via MATHCAD®'s Find Solve Block that uses Equations (3.18), (3.24), (3.26), and (5.4). The root-raised cosine pulses truncated to the same duration gT are superimposed on the graphs for performance comparison purposes.

A. PULSE DURATION $= 5T$, $k_{\max} = 5$, $Y = 0.99$

The simultaneous solution of Equations (3.18), (3.24), (3.26) and (5.4) yields the coefficients c_k and the 0.99 power bandwidth w as shown in Table 7 below,

Table 7 Coefficients c_k for new pulse of duration $5T$ with $k_{\max} = 5$ and $Y = 0.99$.

c_{-5}	$3.3103\times10^{-3} + j8.5453\times10^{-3}$
c_{-4}	$0.0254 + j0.0436$
c_{-3}	$0.0830 + j0.0884$
c_{-2}	$0.1542 + j0.0875$
c_{-1}	$0.1935 + j0.0385$
c_0	0.1997
c_1	$0.1935 + j3.3680\times10^{-4}$
c_2	$0.1579 + j0.0192$
c_3	$0.0885 + j0.0267$
c_4	$0.0285 + j0.0157$
c_5	$3.9247\times10^{-3} + j3.5156\times10^{-3}$
w	$0.7642/T$

Substituting the coefficients c_k results into Equations (3.2) and (3.6) yields $p(t)$ and $\left|P(f)\right|^2$, which are as shown in Figure 17. The root-raised cosine pulse truncated to the same duration $5T$ in equations (2.7) and (2.8) yields $p'_{RC}(t)$ and $\left|P'_{RC}(f)\right|^2$ which are superimposed on the graph for performance comparison. Note, in this case that the first null bandwidth is $1.2/T$ as predicted by Equation (3.28) and the spectral roll-off is -140 dB/decade as predicted by Equation (3.29). The spectral roll-off of this new pulse is substantially better than that of the truncated root-raised cosine pulse. The 0.99 power bandwidth achieved for this pulse design is $0.7642/T$. This value is approximately 16% larger than the 0.99 power bandwidth of the untruncated root raised cosine pulse as shown in Table 11. Recall that the untruncated root raised cosine pulse has infinite duration, and that a truncated root raised cosine pulse will not have as narrow a bandwidth. The infinite duration root raised cosine is used here for comparison because its bandwidth is a lower bound on achievable bandwidth using realizable root raised cosine pulses.

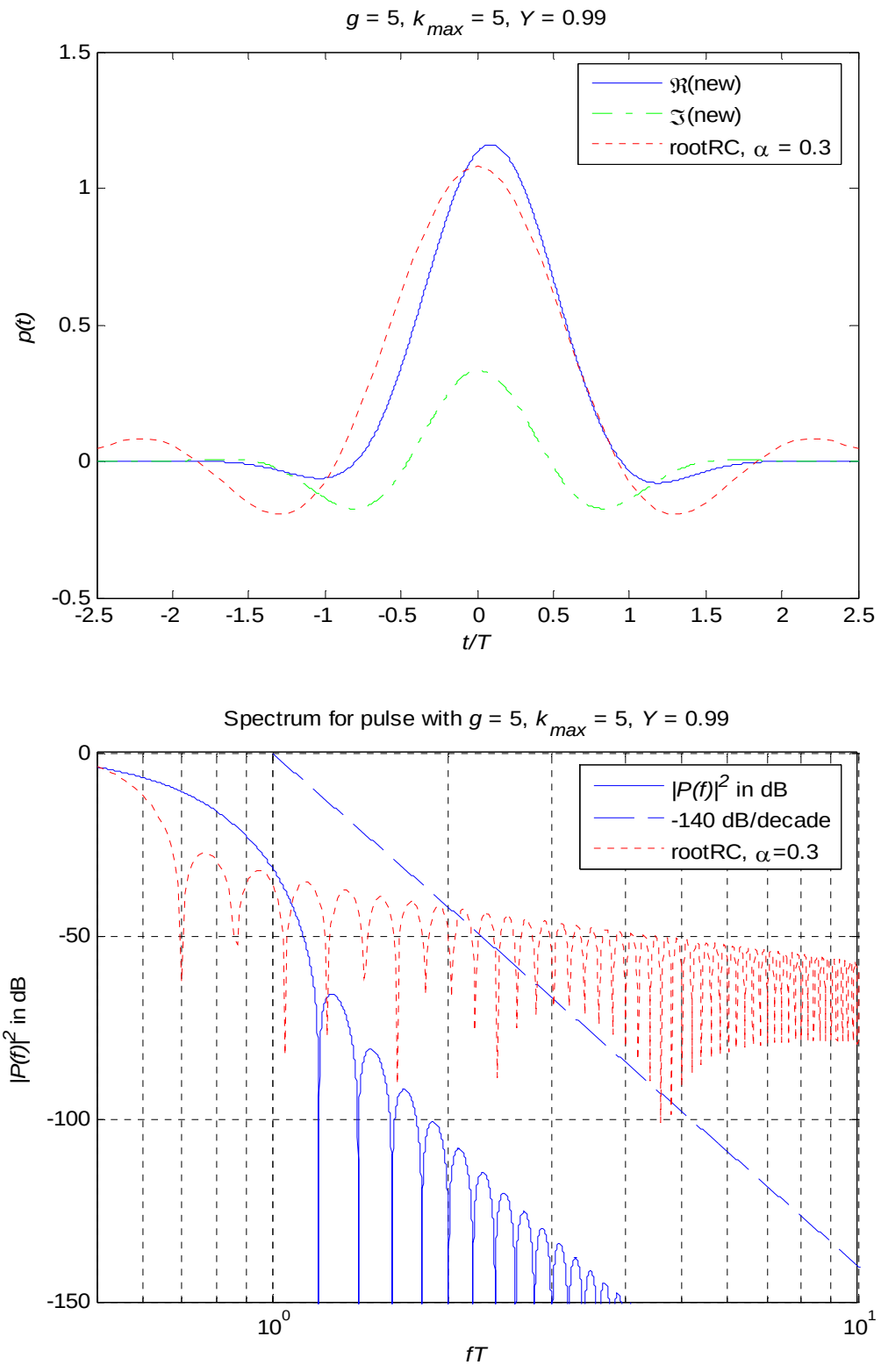

Figure 17 Comparison of duration $5T$, new pulse (with $k_{\max} = 5$, $Y = 0.99$) and truncated root raised cosine (with $\alpha = 0.3$) pulse shapes.

B. PULSE DURATION $= 5T$, $k_{\max} = 4$, $Y = 0.99$

The simultaneous solution of Equations (3.18), (3.24), (3.26) and (5.4) yields the coefficients c_k and the 0.99 power bandwidth w as shown in Table 8 below,

Table 8 Coefficients c_k for new pulse of duration $5T$ with $k_{\max} = 4$ and $Y = 0.99$.

c_{-4}	$0.0119 - j0.0207$
c_{-3}	$0.0588 - j0.0791$
c_{-2}	$0.1337 - j0.1114$
c_{-1}	$0.1882 - j0.0635$
c_0	0.2
c_1	$0.1982 + j0.0119$
c_2	$0.1739 - j7.0730 \times 10^{-3}$
c_3	$0.0976 - j0.0136$
c_4	$0.0234 - j4.9962 \times 10^{-3}$
w	$0.6945 / T$

Substituting this result into Equations (3.2) and (3.6) yields $p(t)$ and $\left|P\left(f\right)\right|^2$, which are as shown in Figure 18. The root-raised cosine pulse truncated to the same duration $5T$ in equations (2.7) and (2.8) yields $p'_{RC}\left(t\right)$ and $\left|P'_{RC}\left(f\right)\right|^2$ which are superimposed on the graph for performance comparison. Note, in this case that the first null bandwidth is $1/T$ as predicted by Equation (3.28) and the spectral roll-off is -100 dB/decade as predicted by Equation (3.29). In contrast to the pulse in Figure 17, we are sacrificing spectral roll-off for improved first null bandwidth performance by reducing $k_{\max}$ from 5 to 4. The spectral roll-off of this new pulse is still substantially better than that of the truncated root-raised cosine pulse even with the trade off between spectral roll-off for improved first null bandwidth performance. The 0.99 power bandwidth achieved for this pulse design is $0.6945/T$. In contrast to the pulse in Figure 17, this value is now only 8% larger than the 0.99 power bandwidth of the untruncated root raised cosine pulse as shown in Table 11. This example demonstrates that for same finite duration new pulses, we can control the $k_{\max}$ to yield the required fractional power bandwidth and spectral roll-off.

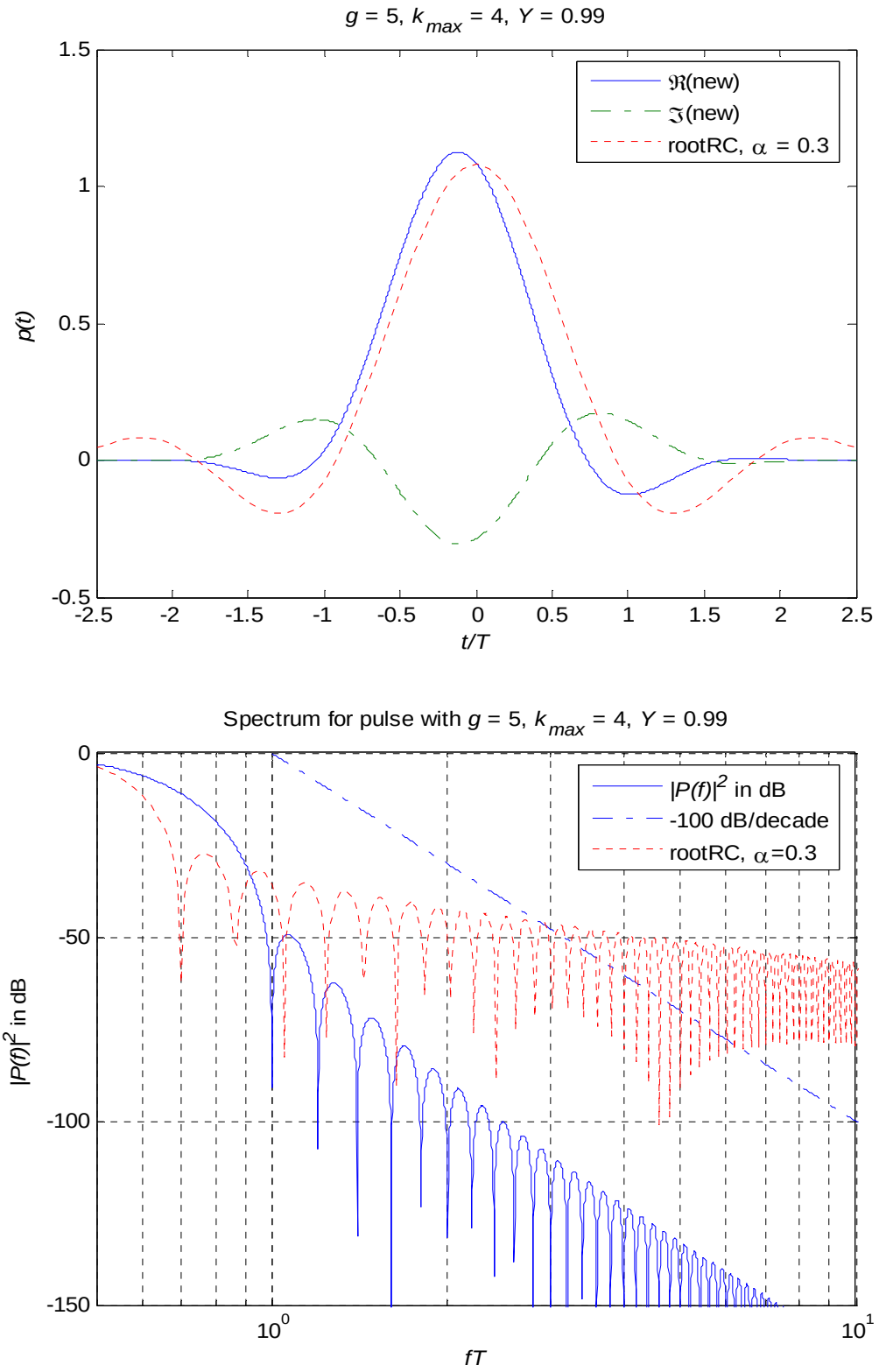

Figure 18 Comparison of duration $5T$, new (with $k_{\max} = 4$ and $Y = 0.99$) and truncated root raised cosine (with $\alpha = 0.3$) pulse shapes.

C. PULSE DURATION $= 8T$, $k_{\max} = 5$, $Y = 0.99$

The simultaneous solution of Equations (3.18), (3.24), (3.26) and (5.4) yields the coefficients c_k and the 0.99 power bandwidth w as shown in Table 9 below,

Table 9 Coefficients c_k for new pulse of duration $8T$ with $k_{\max} = 5$ and $Y = 0.99$.

c_{-5}	$0.0203 + j0.0157$
c_{-4}	$0.0770 + j0.0372$
c_{-3}	$0.1198 + j0.0193$
c_{-2}	$0.1242 - j0.0139$
c_{-1}	$0.1242 - j0.0140$
c_0	0.125
c_1	$0.1249 - j5.7909 \times 10^{-3}$
c_2	$0.1238 - j0.0173$
c_3	$0.1220 - j8.7691 \times 10^{-3}$
c_4	$0.0911 + j1.6375 \times 10^{-3}$
c_5	$0.0300 + j1.1427 \times 10^{-3}$
w	$0.5842 / T$

Substituting this result into Equations (3.2) and (3.6) yields $p(t)$ and $\left|P\left(f\right)\right|^2$, which are as shown in Figure 19. The root-raised cosine pulse truncated to the same duration $8T$ in equations (2.7) and (2.8) yields $p'_{RC}\left(t\right)$ and $\left|P'_{RC}\left(f\right)\right|^2$ which are superimposed on the graph for performance comparison. Note, in this case that the first null bandwidth is $0.75/T$ as predicted by Equation (3.28) and the spectral roll-off is -80 dB/decade as predicted by Equation (3.29). The spectral roll-off of this new pulse is substantially better than that of the truncated root-raised cosine pulse. This is a good example of fairly even balance in the first null bandwidth versus spectral roll-off tradeoff. The 0.99 power bandwidth achieved for this pulse design is $0.5842/T$. This value is approximately 9% better than the ideal best case 0.99 power bandwidth of the untruncated root raised cosine pulse as shown in Table 11. This new pulse outperforms the root raised cosine pulse in terms of both the 0.99 power bandwidth and the spectral roll-off.

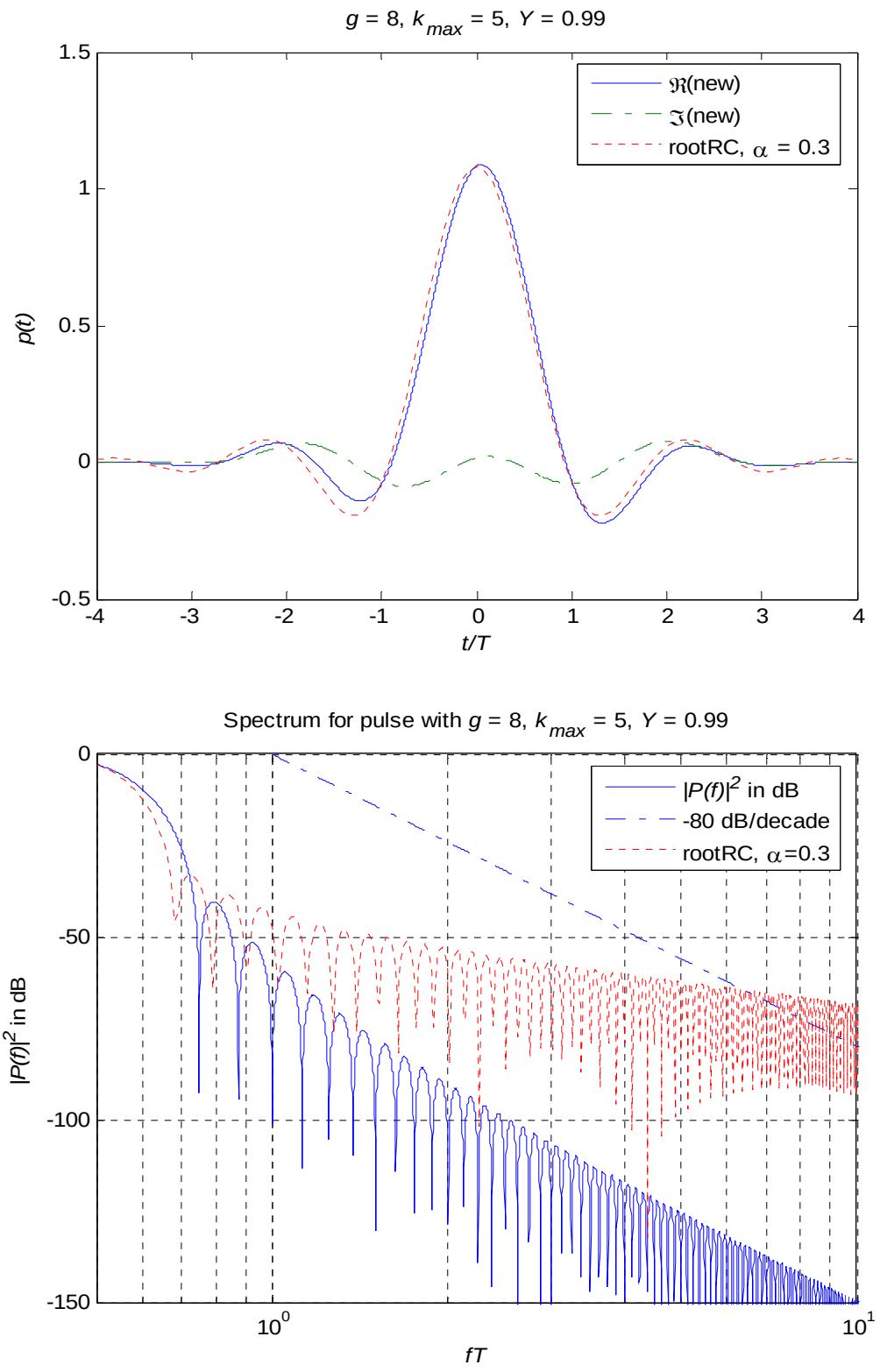

Figure 19 Comparison of duration $8T$, new (with $k_{\max} = 5$ and $Y = 0.99$) and truncated root raised cosine (with $\alpha = 0.3$) pulse shapes.

D. PULSE DURATION $= 8T$, $k_{\max} = 4$, $Y = 0.99$

The simultaneous solution of Equations (3.18), (3.24), (3.26) and (5.4) yields the coefficients c_k and the 0.99 power bandwidth w as shown in Table 10 below,

Table 10 Coefficients c_k for new pulse of duration $8T$ with $k_{\max} = 4$ and $Y = 0.99$.

c_{-4}	$0.0864 + j0.0187$
c_{-3}	$0.1218 - j0.0280$
c_{-2}	$0.1104 - j0.0587$
c_{-1}	$0.1236 - j0.0188$
c_0	0.1250
c_1	$0.1210 - j0.0313$
c_2	$0.1126 - j0.0542$
c_3	$0.0685 - j0.1045$
c_4	$5.6675 \times 10^{-4} - j0.0884$
w	$0.5420 / T$

Substituting this result into Equations (3.2) and (3.6) yields $p(t)$ and $\left|P\left(f\right)\right|^2$, which are as shown in Figure 20. The root-raised cosine pulse truncated to the same duration $8T$ in equations (2.7) and (2.8) yields $p'_{RC}\left(t\right)$ and $\left|P'_{RC}\left(f\right)\right|^2$ which are superimposed on the graph for performance comparison. Note, in this case that the first null bandwidth is $0.625/T$ as predicted by Equation (3.28) and the spectral roll-off is -40 dB/decade as predicted by Equation (3.29). In contrast to the pulse in Figure 19, this example illustrates that by sacrificing the spectral roll-off of this pulse to itself being continuous, implying its second derivative is impulsive, the pulse has smaller first null bandwidth compared to the truncated root-raised cosine pulse of the same duration. The 0.99 power bandwidth achieved for this pulse design is $0.5420/T$. In contrast to the pulse in Figure 19, this value is 18% better than the 0.99 power bandwidth of the untruncated root raised cosine pulse as shown in Table 11. This new pulse outperforms the root raised cosine pulse in term of the 0.99 power bandwidth, the first null bandwidth, and the spectral roll-off.

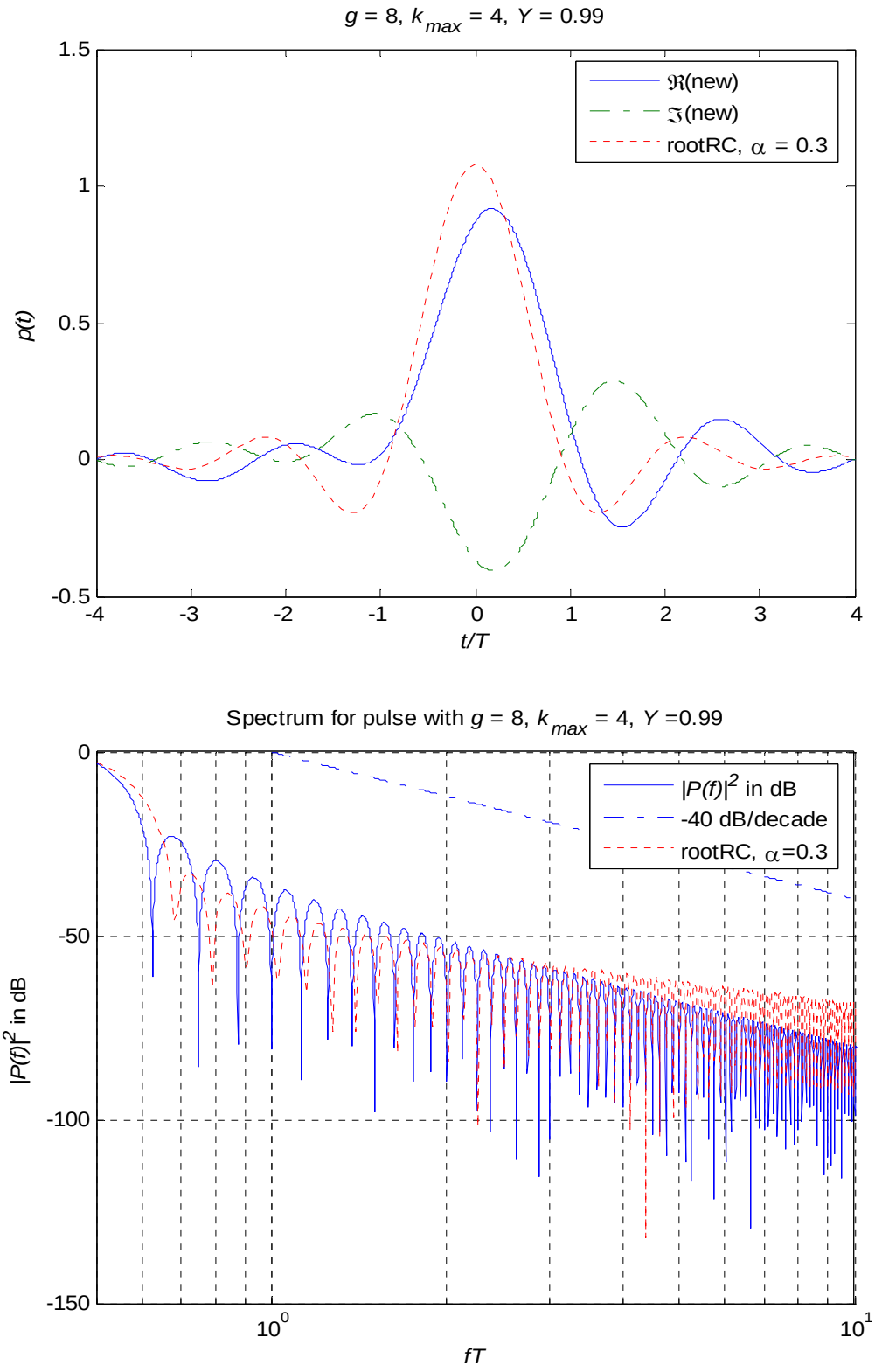

Figure 20 Comparison of duration $8T$, new (with $k_{\max} = 4$ and $Y = 0.99$) and truncated root raised cosine (with $\alpha = 0.3$) pulse shapes.

E NEW PULSES FRACTIONAL POWER BANDWIDTH PERFORMANCE

Table 11 below shows favorable spectral occupancy of these new pulses for each g and $k_{\max}$. The 0.90, 0.95 and 0.99 power bandwidths are less than its corresponding first null bandwidth. Additionally, we observed that at 0.90 power, the new pulses from $g = 5, k_{\max} = 4$ onwards outperformed the untruncated root raised cosine pulse in term of fractional power bandwidth. The new pulse at $g = 8, k_{\max} = 4$ also outperformed the untruncated root raised cosine pulse in all listed bandwidth criteria.

Table 11 Comparison of first null bandwidth and fractional power bandwidth w for varied g and $k_{\max}$, and untruncated root raised cosine with $\alpha = 0.3$.

	$g = 2$ $k_{\max} = 2$	$g = 3$ $k_{\max} = 3$	$g = 4$ $k_{\max} = 4$	$g = 5$ $k_{\max} = 5$	$g = 5$ $k_{\max} = 4$
First Null bandwidth	$1.5/T$	$1.3333/T$	$1.25/T$	$1.2/T$	$1/T$
0.90 power bandwidth	$0.6886/T$	$0.6062/T$	$0.5658/T$	$0.5447/T$	$0.5131/T$
0.95 power bandwidth	$0.8040/T$	$0.7020/T$	$0.6503/T$	$0.6232/T$	$0.5800/T$
0.99 power bandwidth	$1.0095/T$	$0.8721/T$	$0.8000/T$	$0.7642/T$	$0.6945/T$

	$g = 8$ $k_{\max} = 5$	$g = 8$ $k_{\max} = 4$	**untruncated root RC with** $\alpha = 0.3$
First Null bandwidth	$0.75/T$	$0.625/T$	$0.66/T$
0.90 power bandwidth	$0.4667/T$	$0.4543/T$	$0.5385/T$
0.95 power bandwidth	$0.5119/T$	$0.4895/T$	$0.5933/T$
0.99 power bandwidth	$0.5842/T$	$0.5420/T$	$0.6383/T$

F. NEW PULSES WITH FRACTIONAL POWER BANDWIDTH CONTAINMENT INTERSYMBOL INTERFERENCE PERFORMANCE

The following new pulses with the corresponding coefficients c_k are used in this section's analysis. Note that x^T implies the transpose of x.

Table 12 New pulses' coefficients c_k for fractional power bandwidth containment ISI analysis.

New pulse with duration $2T$, $k_{\max} = 2$, and $Y = 0.99$	$(c_{-2}, c_{-1}, \ldots c_2) = \begin{pmatrix} 0.0791 + j0.0791 \\ 0.3162 + j0.1581 \\ 0.4743 \\ 0.3162 - j0.1581 \\ 0.0791 - j0.0791 \end{pmatrix}^T$
New pulse with duration $3T$, $k_{\max} = 3$, and $Y = 0.99$	$(c_{-3}, c_{-2}, \ldots c_3) = \begin{pmatrix} 0.0371 - j0.0144 \\ 0.1538 - j0.0578 \\ 0.2809 - j0.0722 \\ 0.3285 \\ 0.2809 + j0.0722 \\ 0.1538 + j0.0578 \\ 0.0371 + j0.0144 \end{pmatrix}^T$
New pulse with duration $4T$, $k_{\max} = 4$, and $Y = 0.99$	$(c_{-4}, c_{-3}, \ldots c_4) = \begin{pmatrix} 9.0056 \times 10^{-4} - j0.0157 \\ 0.0165 - j0.0786 \\ 0.0810 - j0.1571 \\ 0.1899 - j0.1414 \\ 0.2490 \\ 0.1899 + j0.1414 \\ 0.0810 + j0.1571 \\ 0.0165 + j0.0786 \\ 9.0055 \times 10^{-4} + j0.0157 \end{pmatrix}^T$
New pulse with duration $5T$, $k_{\max} = 5$, and $Y = 0.99$	See Section A of this chapter for this pulse's coefficients c_k

Unsurprisingly, the new pulse achieves zero ISI as its normalized eye pattern takes on the values of ± 1 at the vertical axis when time t is an integer multiple of T as shown in Figure 21, Figure 22, Figure 23, and Figure 24 with varied g and $k_{\max}$ (see Table 12 for the respective coefficients c_k). Additionally, the horizontal openings are still within $\pm 0.3T$, thus indicating minimal impact in terms of sensitivity to jitter.

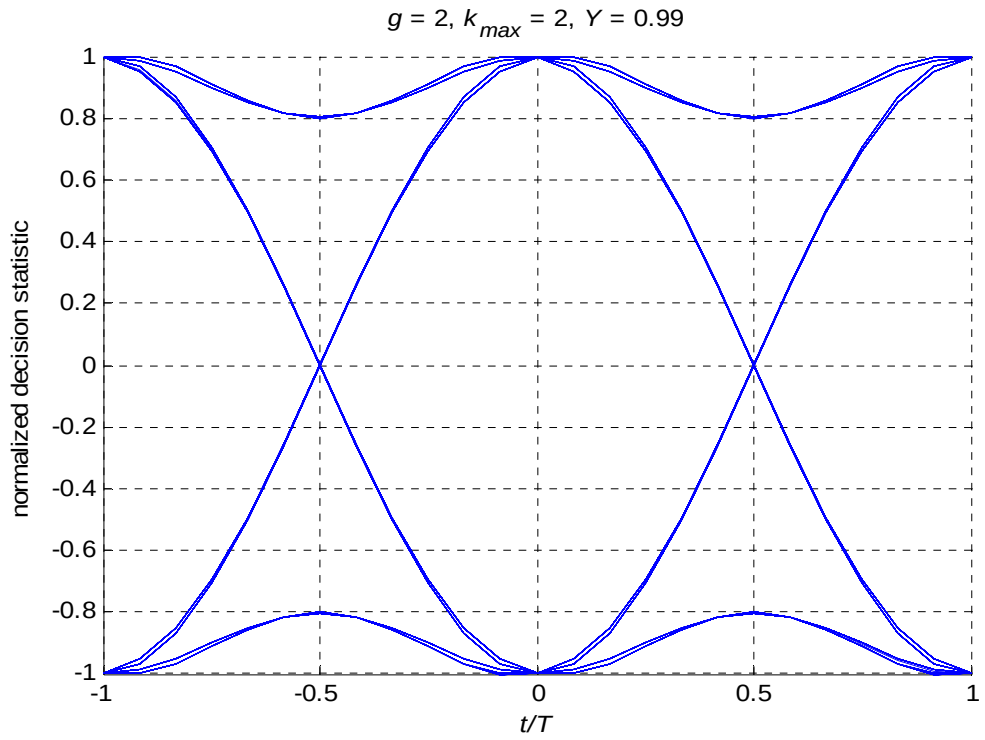

Figure 21 Eye diagram of waveform at the matched filter output for system using the new pulse with duration $2T$ and $Y = 0.99$.

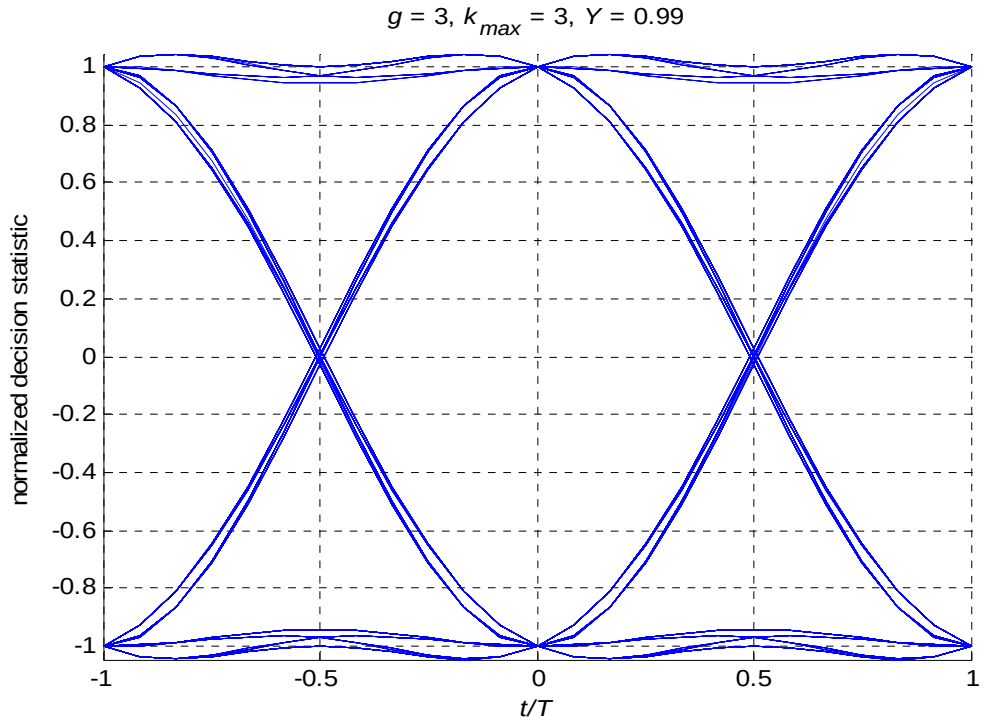

Figure 22 Eye diagram of waveform at the matched filter output for system using the new pulse with duration $3T$ and $Y = 0.99$.

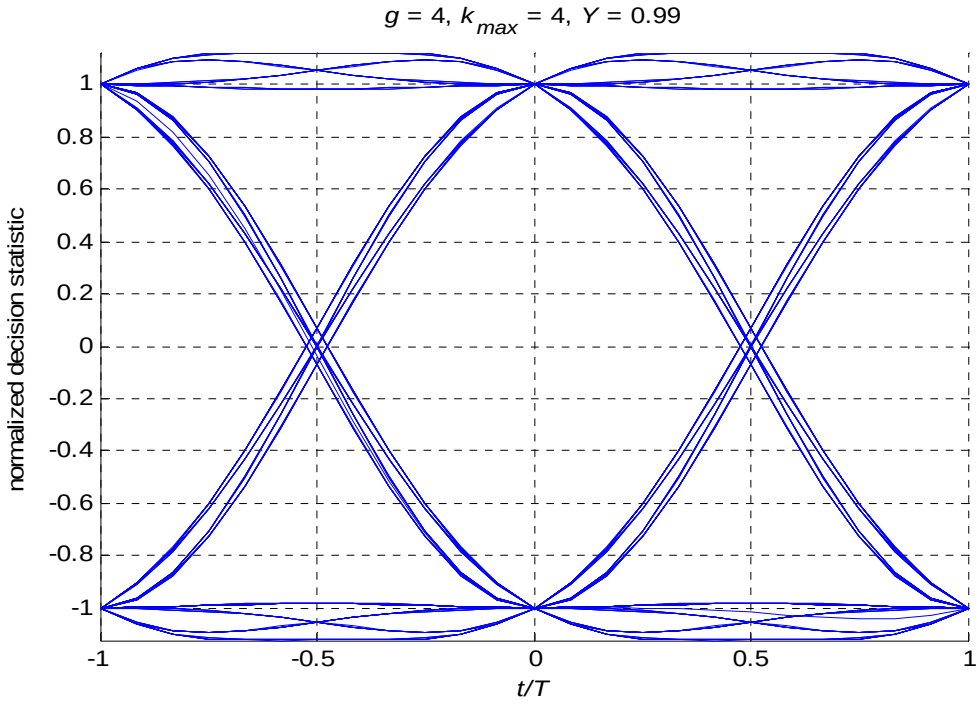

Figure 23 Eye diagram of waveform at the matched filter output for system using the new pulse with duration $4T$ and $Y = 0.99$.

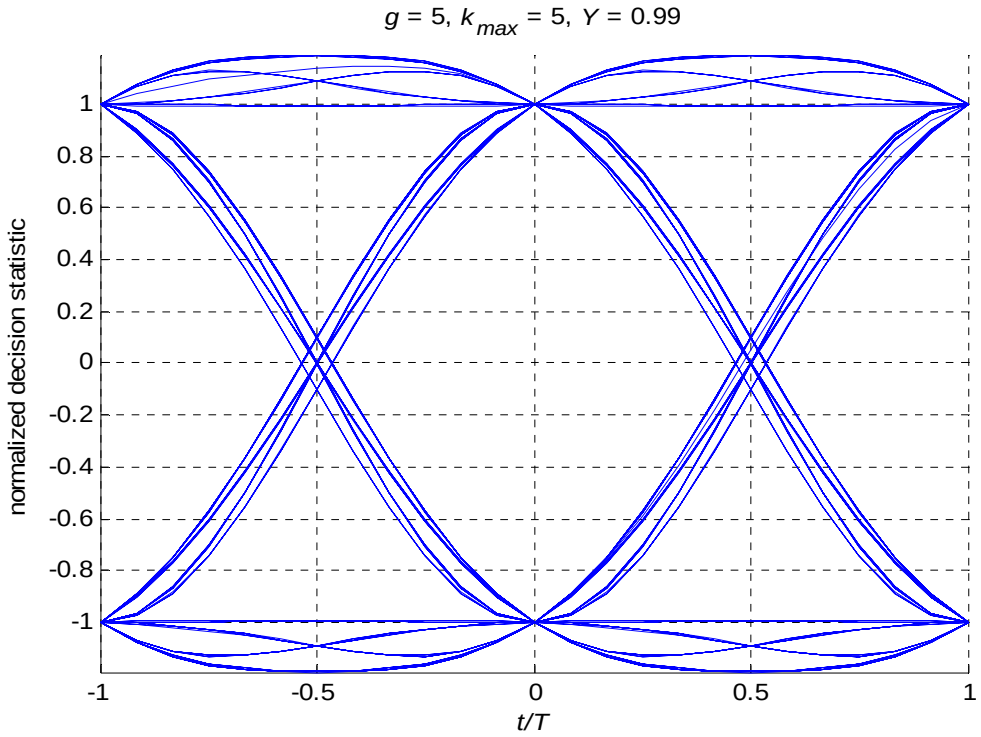

Figure 24 Eye diagram of waveform at the matched filter output for system using the new pulse with duration $5T$ and $Y = 0.99$.

Beyond these presented pulses, there are indeed many permutations and combinations of g and $k_{\max}$ available to devise an appropriate pulse for a required digital communications application. If the fractional power bandwidth constraint is included in the design of the pulses, excellent combinations of pulse durations, fractional power bandwidths and spectral roll off can be achieved.

The next chapter (Chapter VI) concludes this thesis and recommends additional work in this area.

THIS PAGE INTENTIONALLY LEFT BLANK

VI. CONCLUSION

This thesis shows a methodology to design pulses for use in radio digital communications systems involving modulations such as PSK or QAM when spectral efficiency is important, such as is often the case for military radio communications systems tasked with the transmission of intelligence, surveillance, and reconnaissance information. The pulses were designed to have finite duration, first null bandwidth as well as fractional power bandwidth between half the symbol rate $(0.5/T)$ and the symbol rate $(1/T)$ and to achieve the optimum spectral roll-off for a given first null bandwidth. Additionally, these pulses exhibit zero ISI and low susceptibility to jitter. The methodology is very general and can result in an infinite number of combinations of pulse durations, first null bandwidths, fractional power bandwidth, and spectral roll-offs, giving the designer a large trade space in which to trade one parameter against another to achieve design goals. Furthermore, the design methdology can be easily altered to include additional design criteria. Design examples were first illustrated in Chapter IV, with excellent combinations of first null bandwidths and spectral roll-off. More design examples were illustrated in Chapter V, including excellent design combinations of fractional power bandwidth and spectral roll-off. The spectral occupancy of these pulses was compared with that of root raised cosine pulses truncated to the same length with favorable results.

Since Equation (3.18) is quadratic in c_k and since our solutions are only approximate, there is no guarantee, and indeed it is unlikely, that the solutions presented herein are unique. More work is needed to determine if simpler pulses can match the spectral desirability of those found in Chapter IV, for the same pulse duration (gT) and the same number of Fourier components $(2k_{\max}+1)$. It would be wise to see if the design algorithm of Chapter V, which calculates the fractional power bandwidth could be modified to constrain the fractional power bandwidth, perhaps resulting in pulses with even improved fractional power bandwidth. Investigation into the application of the additional constraint of low variation of instantaneous power, would be very interesting due to the deleterious effects of non-linear power amplifiers upon signals with high

instantaneous power, as found in many communications systems. Further, it would be wise to investigate the practicality of generating these pulses in practical transmitters, as well as design of the corresponding matched filters for receivers. Examples of relevant issues to consider include pulse fidelity versus number of samples per pulse, computational complexity, and ease or difficulty of synchronization.

Since the root raised cosine pulse shape is in common use in many operating communications systems, including expensive military satellite communications systems, and since the pulses presented herein offer superior spectral efficiency, it seems wise to pursue this methodology further. Such increases in spectral efficiency offer the potential for enhanced information connectivity across the battlespace, potentially at a reduced cost.

LIST OF REFERENCES

[1] J. G. Proakis, Digital Communications. New York: McGraw Hill, 4 ed., 2001.

[2] J. G. Proakia, M. Salehi, and G. Bauch, Contemporary Communication Systems using MATLAB®. Thomson Brooks/Cole, 2 ed., 2004.

[3] D. J. Hermes and F. E. Kragh, "A bandwidth efficient constant envelope modulation," in Proceedings of the Asilomar Conference on Signals, Systems, and Computers, (Pacific Grove, California), IEEE, Oct. 2006.

[4] L. P. Riddle, "Computation of spectrally efficient pulse shapes in satellite communication," in Proceedings of the Global Telecommunications Conference (GlobeCom), pp. 2056–2060, IEEE, 1990.

[5] C. Park and J. H. Lee, "New bandwidth efficient overlapped pulse shape," IEE Electronics Letters, vol. 31, no. 23, pp. 1975–1976, 1995.

[6] D. Slepian and H. O. Pollak, "Prolate spheroidal wave functions, Fourier analysis and uncertainty - I," Bell System Technical Journal, vol. 40, pp. 43–64, 1961.

[7] F. E. Kragh, C. W. Nga, D. J. Hermes and R. C. Robertson, "Spectrally efficient digital modulation using new pulse shapes," in Proceedings of Military Communications Conference, IEEE, 2007.

[8] R. N. Bracewell, Fourier Transform and its Applications. New York: McGraw Hill, 3 ed., 1999.

[9] B. Sklar, Digital Communications: Fundamentals and Applications. Upper Saddle River, New Jersey: Prentice Hall, 2 ed., 2001.

[10] M. B. Pursley, Introduction to Digital Communications. Upper Saddle River, New Jersey: Prentice Hall, 2003.

[11] A. Goldsmith, Wireless Communications. New York: Cambridge University Press, 2005.

THIS PAGE INTENTIONALLY LEFT BLANK

INITIAL DISTRIBUTION LIST

1. Defense Technical Information Center
   Ft. Belvoir, Virginia

2. Dudley Knox Library
   Naval Postgraduate School
   Monterey, California

3. Professor Jeffrey Knorr, Chairman, Code EC
   Department of Electrical and Computer Engineering
   Naval Postgraduate School
   Monterey, California

4. Assistant Professor Frank Kragh, Code EC/Kh
   Department of Electrical and Computer Engineering
   Naval Postgraduate School
   Monterey, California

5. Professor Roberto Cristi, Code EC/Cx
   Department of Electrical and Computer Engineering
   Naval Postgraduate School
   Monterey, California

6. Donna Miller, Code EC
   Department of Electrical and Computer Engineering
   Naval Postgraduate School
   Monterey, California

7. Captain John Pope
   Program Manager, Satellite Communications
   PEO C4I and Space
   San Diego, California

8. Dr. Roy Axford
   Space and Naval Warfare Systems Center
   San Diego, California

9. Ray Cole
   Networks and Communication Systems Branch
   U.S. Naval Research Laboratory
   Washington, DC